GENERAL ELECTRIC

GENERAL ELECTRIC COMPANY
CORPORATE RESEARCH AND DEVELOPMENT
Schenectady, N.Y.

CARBON AND GRAPHITE SCIENCE

by

D. W. McKee, Physical Chemistry Laboratory

Report No. 72CRD319 November 1972

TECHNICAL INFORMATION SERIES

CLASS 1

GENERAL ELECTRIC

General Electric Company
Corporate Research and Development
Schenectady, New York

TECHNICAL INFORMATION SERIES

AUTHOR	SUBJECT	NO.
McKee, DW	carbon	72CRD319
		DATE: November 1972
TITLE: Carbon and Graphite Science		GE CLASS: 1
		NO. PAGES: 24
ORIGINATING COMPONENT: Physical Chemistry Laboratory		CORPORATE RESEARCH AND DEVELOPMENT SCHENECTADY, N.Y.

SUMMARY: This is a brief review of the properties and structure of the newer forms of carbon and a summary of recent studies of the chemical reactivity of graphite surfaces. This report is also a contribution to the series, "Annual Review of Material Science."

KEY WORDS: carbon, graphite, fibers, whiskers

INFORMATION PREPARED FOR _____

Additional Hard Copies Available From

Corporate Research & Development Distribution
P.O. Box 43 Bldg. 5, Schenectady, N.Y., 12301

Microfiche Copies Available From

Technical Information Exchange
P.O. Box 43 Bldg. 5, Schenectady, N.Y., 12301

CARBON AND GRAPHITE SCIENCE

D. W. McKee

INTRODUCTION

Carbon covers such a wide spectrum of materials and the science of carbon embraces so many diverse disciplines that it would obviously be impossible and undesirable to attempt to review advances in this vast field in one brief report. Any selection of topics must therefore be arbitrary and reflects the personal interests and enthusiasms of the author. From this limited standpoint, two major developments in carbon and graphite science appear to have taken place over the past five years: the emergence of new forms of carbon with excitingly novel structures and mechanical properties and the application of microscopic methods, at several levels of sophistication, to the study of the reactivity of carbon and graphite surfaces. The first development is bringing about a revolution in the field of materials and composites, while the second is shedding much needed light on the complex and important area of the surface chemistry of carbon.

These two areas, though apparently unrelated, have more in common than appears at first sight. The technological applications of the new carbon materials are currently limited to a large extent by the surface state of the carbonaceous phase and its reactivity towards gaseous environments at elevated temperatures.

This report will therefore be divided into two parts: a discussion of the properties and structures of new physical forms of carbon developed during the past five years, and a survey of recent advances in the area of graphite reactivity in gaseous environments. No attempt will be made at encyclopedia coverage of either area--rather the more recent highlights of interest to the materials scientist will be emphasized. Unfortunately, for space reasons, there can be no discussion of such interesting older fields as pyrolytic carbon, graphite intercalation compounds or of advances in the understanding of the purely physical properties of graphite, and diamond. These topics have been the subjects of recent reviews and will no doubt be covered in later volumes of this series.

GRAPHITE WHISKERS

Preparation

Although filamentous forms of carbon and graphite have been known for some time, the controlled preparation of high-strength graphite whiskers is a more recent development. Bacon[1] has grown graphite whiskers by forming a d-c arc between carbon electrodes under an argon pressure of 92 atm at temperatures near the sublimation point of graphite (3900°K). Graphite vaporized from the tip of the positive electrode and deposited as a cylindrical boule in which whiskers of up to 3 cm in length and a few microns in diameter were embedded.

Whiskers and filaments of graphite have often been observed to form during pyrolytic deposition processes; for example, during the thermal decomposition of acetylene on Nichrome wires below 700°C,[2] during the pyrolysis of methane,[3] n-heptane,[4] and CO[5] on iron surfaces at elevated temperatures and on heated carbon filaments.[6] Because metal particles have often been detected near the growing ends of the filaments, whisker growth is generally regarded as being catalyzed by metals, especially by iron[7] which appears to be more active in promoting whisker growth than other metal substrates. Whiskers have also been observed growing on natural Ticonderoga graphite crystals.[8]

Structure

Graphite whiskers exhibit basically two types of structural orientation. Those produced by the pyrolytic decomposition of hydrocarbons and CO generally have the graphite layers oriented parallel to the substrate surface, as is the case with pyrolytic graphite. However, the secondary growth of pyrolytic graphite layers may disturb the orientation of the original filament. Whiskers on natural graphite crystals are oriented with the (0001) planes perpendicular to the whisker axis, probably as a result of spiral growth around a screw dislocation.[8] The hollow filaments produced by Hillert and Lange[4] by n-heptane pyrolysis showed the opposite orientation, with the c-axis perpendicular to the whisker axis. This is most likely the result of initial growth of the graphite layers parallel to the surface of a catalyst particle. Intermediate orientation with basal planes at an angle of 30° to the axis have been reported for whiskers growing on carbon fibers.[6] Bacon's whiskers[1] consist of graphite sheets several angstroms thick rolled in concentric layers so that the c-axis is strictly normal to the whisker axis.[9] Solid, hollow, and ribbon-like structure can also be found in deposits of this type.

Mechanical Properties

Although whiskers made by pyrolytic deposition tend to be weak, the scroll-like structure of the whiskers made by the d-c arc method of Bacon and the orientation of the graphite basal planes parallel to the whisker axis result in mechanical properties which approach the theoretical values for the graphite lattice. Maximum tensile strengths of 2.85×10^6 psi and elastic moduli greater than 100×10^6 psi have been reported.[1] Unfortunately, owing to the expense and difficulty of preparation, these whiskers have not found commercial application and in recent years more attention has been paid to high-strength carbon fibers prepared from synthetic organic precursors.

Manuscript received November 20, 1972

HIGH-STRENGTH CARBON FIBERS

Carbon fibers made by the pyrolysis of fibrous polymers have been known for a considerable time although it is only recently that their mechanical properties have been improved sufficiently to make them attractive engineering materials. Since the process for making these fibers from polyacrylonitrile (PAN) precursor was announced about five years ago, there has been an explosive growth of interest in this area, in spite of the fact that substantial markets for these novel materials have yet to be developed. The immediate future of high-strength carbon fibers appears to lie in the area of structural composites, although there are promising new applications (e. g. , in carbon brush technology) where unbonded fibers can be utilized. Because of their unique structure and properties the new carbon fibers are of considerable scientific interest, and it is with these aspects that this discussion will be primarily concerned.

Preparation and Chemistry of Formation

The processes involved in the transformation of PAN to high-strength carbon fibers have recently been reviewed by Watt. [10] In the basic process, developed at the Royal Aircraft Establishment, Farnborough, England, bundles or "tows" of PAN fibers are wound onto frames to prevent shrinkage and are then heated in an air oven at 220°C for a few hours. The fibers are then removed from the frames, carbonized at 1000°C in an inert atmosphere, and then given a final heat treatment at 1500° to 2500°C. The mechanical properties of the fibers dramatically improve during the final stage; but whereas the modulus continues to rise with increasing heat treatment temperature, the tensile strength passes through a maximum value at about 1500°C. Two different types of fiber are now available, according to the heat treatment conditions used in their fabrication. These are generally referred to as Type I (treated to above 2000°C, high modulus ca. 55×10^6 psi, low strength ca. 250,000 psi) and Type II (treated to 1500°C or below, low modulus ca. 35×10^6 psi, high strength ca. 400,000 psi). High modulus fibers can also be made by stretching unoxidized PAN fibers during the carbonization process and also by high-temperature stretching after carbonization.

The PAN structure (Fig. 1A) is basically a polyethylene chain with a CN group on alternate C atoms. On heating in air at 220°C a ladder polymer is formed with, according to Watt, [11] ketonic groups attached to the carbon chain (Fig. 1B). On heating to above 300°C, water, HCN, and then nitrogen are eliminated to give a fused ring structure (Fig. 1C) which loses hydrogen at still higher temperatures to form a hexagonal network of carbon atoms (Fig. 1D). The critical temperature for the formation of this carbon network appears to be about 700°C. [12] In order to achieve a high modulus in the final fiber it is necessary to maintain the fibers under tension during the oxidation stage, so that the polymer chain orientation is not relaxed. In the case of rayon-based

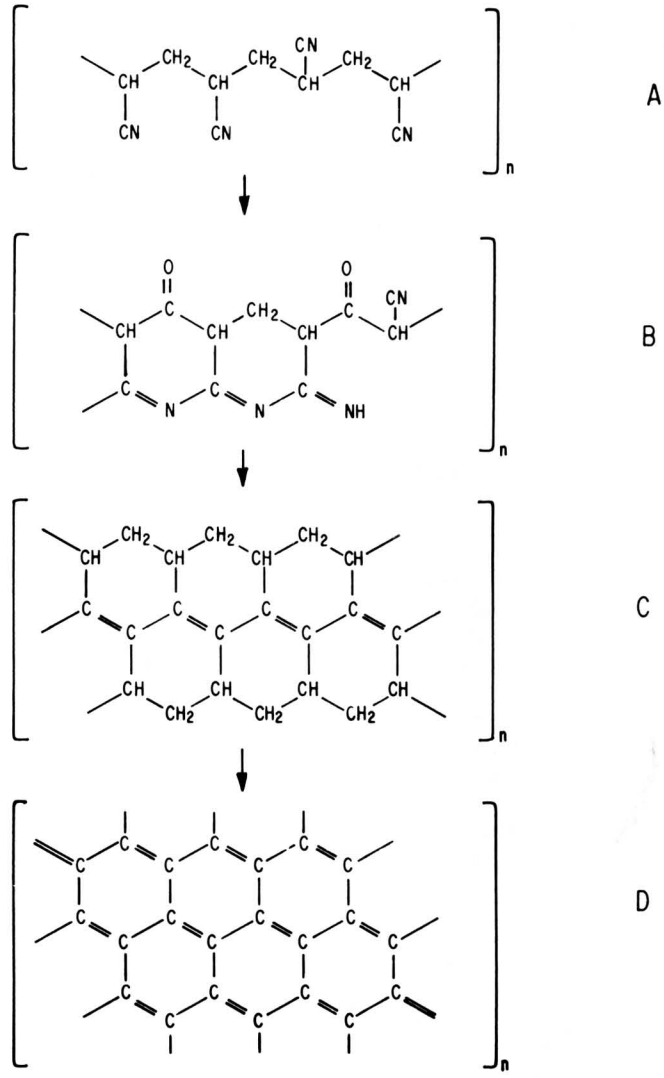

Fig. 1 Formation of carbon fiber from PAN, according to Watt. [11] A. PAN structure. B. Oxidized PAN ladder polymer. C. Condensed ring system. D. Final graphitic network.

fibers, tension is applied at temperatures above 2700°C so that the crystalline orientation is increased as a result of plastic flow.

There is still much doubt concerning the exact nature of the complex reactions that occur during the oxidation stage with PAN-based fibers. Although Watt [11] believes that CO bonds are formed, others have found evidence for the formation of ether linkages, [13] free radicals, [14] or hydroxyl bonds. [15] Bailey and Clarke [15] have suggested that hydrogen bonding may play a role in determining the mechanical properties of the oxidized fibers. It also appears that the oxidation process itself can be replaced by a sulfurization or nitrosation step. [16]

A number of other precursor materials have been used to produce carbon fibers of high strength and modulus, although PAN and rayon remain the preferred polymers for optimum mechanical properties. Isotropic fibers of glassy carbon have been prepared by Yamada and Yamamoto[17] from resin mixtures; however, even after graphitization at 2700°C, the orientation remained very low and the structure was essentially that of glassy carbon. Tensile strengths of 150,000 psi and moduli of up to 10×10^6 psi have been reported for this material More recently the carbonization of a phenolic resin fiber to yield a glassy carbon fiber has been described.[18] By applying tension during carbonization at 800°C some orientation could be induced in the structure, but only a slight increase in modulus was attained. Low-temperature (800°C) stretching followed by high-temperature stretching between 2000° and 2750°C produced a further increase in overall orientation and an increase in modulus from 4 to 24.5×10^6 psi.

Moderately high strength fibers have also been prepared from pitch.[19] However, these fibers still possessed an isotropic structure even after stretching at temperatures up to 2600°C. With some pitch precursor materials a fair degree of preferred orientation can be induced, although the mechanical properties have to date always proved inferior to those of PAN-based fibers. More recently better quality, highly oriented fibers have been produced from asphalt.[20] These showed tensile strengths as high as 375,000 psi and moduli of 70×10^6 psi following stress graphitization at 2000° to 2800°C. Finally, carbon fibers have been prepared by the thermal decomposition of vinylidene chloride/vinyl chloride copolymer (Saran).[21] The polymer can be pyrolyzed slowly by raising the temperature to 850°C at 50°C/hr and maintaining this temperature for 12 hours, followed by graphitization at 2500°C under tension. The best mechanical properties (tensile strength 55,000 psi, modulus 4×10^6) are once again much inferior to those of the PAN-based product, probably because of the large volumes of gaseous decomposition products which are evolved from Saran on pyrolysis, resulting in a porous fiber of low density.

Structure

As a result of much detailed (but often repetitive) work a fairly complete picture of the unique structural features of high-strength carbon fibers and the conditions of formation necessary for optimum mechanical properties has emerged during the past five years. In a general way, the existence of high-strength carbon fibers depends on the distinction between graphitizing and nongraphitizing carbons. With increasing heat treatment temperature, the physical properties of graphitizing carbons gradually approach those of the ideal graphite lattice, whereas nongraphitizing carbons are less affected and do not possess the necessary orientation to form high-strength fibers. Graphitization is, however, normally preceded by the formation of a viscous phase and the growth of randomly oriented crystallites. In the formation of high-strength fiber from PAN, melting and the formation of three-dimensional graphite are prevented by means of the oxidation treatment under tension which keeps the molecular chains from relaxing during subsequent heat treatment. PAN appears to have a special advantage as a precursor polymer as, because of its ladder structure, hot stretching above 2500°C is not essential. Other fibers, such as cellulose, pyrolyze to a glassy carbon if the hot stretching procedure is omitted.

Two somewhat contradictory views on the fine structure of high-strength carbon fibers have been put forward, respectively, by D. J. Johnson at Leeds and by W. Ruland in Brussels, both models being based on convincing experimental evidence. By using low angle x-ray diffraction analysis[22] and, more recently, high resolution electron microscopy,[23-25] Johnson, Tyson, Crawford, and Oates have proposed a complex structure for PAN-based carbon fibers involving a network of interlinked graphite crystallites separated by low angle tilt and twist boundaries. Lattice resolution micrographs show single extinction bands attributable to nonbasal edge dislocations and boundaries of tilt and twist character. Periodic bands are also observed due to Moiré effects from overlapping crystallites. Experiments with samples tilted in the electron beam show that the layer planes either twist continuously about the fiber axis or bend sharply by means of twist boundaries. A schematic representation of high-strength carbon fiber, according to this model is shown in Fig. 2, which illustrates the lamellar nature of the structure and the occurrence of subgrain boundaries and various types of lattice imperfections. According to Johnson and Crawford,[24] these defects play a major role in determining the mechanical properties of the fibers.

Support for this model can be found in the results of several other structural investigations. J. W. Johnson, Rose, and Scott[26] studied the effect of partial oxidation of PAN on the subsequent structure of the carbon fiber and concluded that the stable structure is basically lamellar rather than fibrillar. The presence of grain boundaries was also suggested as the limiting factor in fiber strength by Williams, Steffens, and Bacon.[27] Wicks[28] used electron diffraction to study the fine structure of PAN-based carbon fibers which had been flame polished with a hydrogen-oxygen mixture. The structure consisted mainly of turbostratic graphite crystallites with the basal layers randomly oriented along the c-axis. Following high-temperature treatment, stacks of graphitic crystallites formed distinct parallel ribbons which enclosed a network of elongated pores. Transverse tilt boundaries between individual crystallites in the ribbons were identified and the average size of the crystallite stacks was generally larger around lenticular voids than in the body of the fiber, probably as a result of impurity segregation which catalyzed the growth of three-dimensionally ordered graphite.

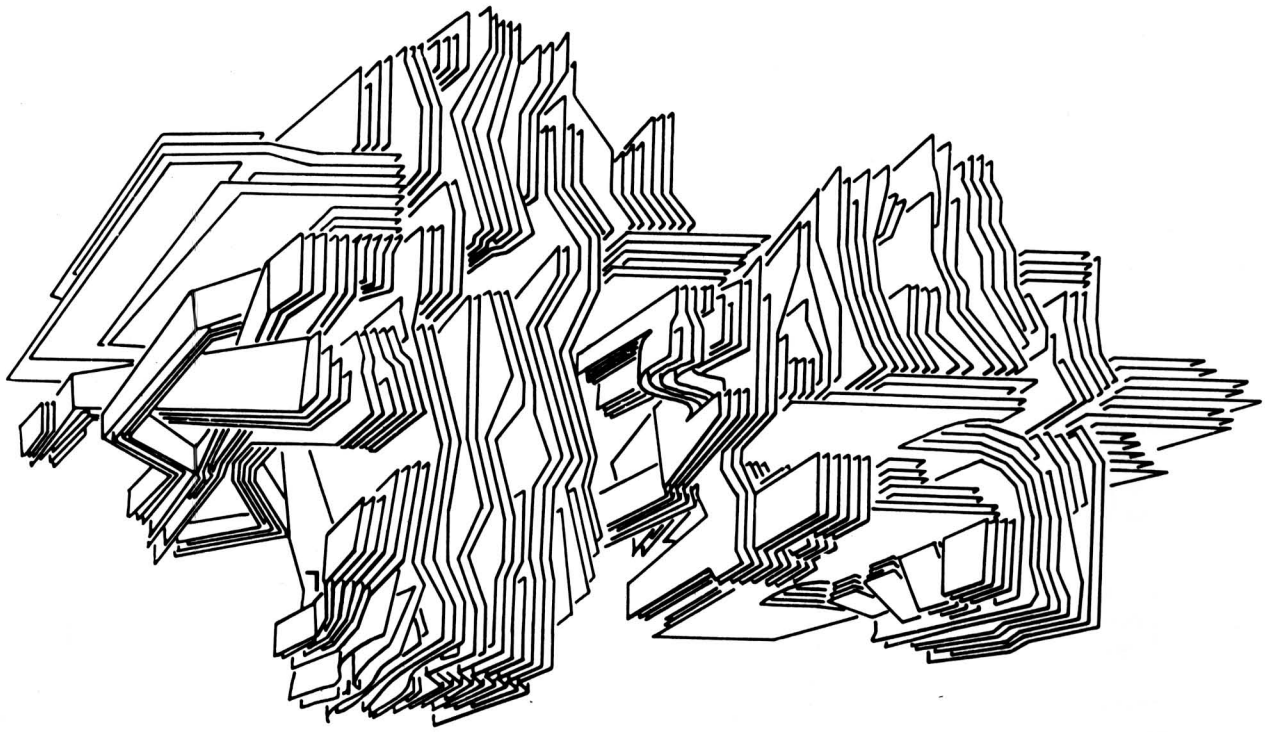

Fig. 2 Structure of high-strength carbon fiber, according to D. J. Johnson [from Crawford and Johnson[24]].

A more uniform and somewhat more idealized fibrillar structure for high-strength carbon fibers has been proposed by Ruland, Fourdeux, and Perret[29-31] on the basis of x-ray scattering and electron diffraction analysis. The microstructure of PAN-based fiber appears to be essentially the same as that of rayon-based fiber, the difference being mainly in the volume fraction occupied by voids, which is considerably lower with the PAN-based material. In both cases, according to this model, the carbon layers are present in the form of long ribbons, the average width of which is 50Å to 70Å depending on the heat treatment conditions. The ribbons are slowly undulating and show long, straight regions of 60Å to 130Å in length. Numbers of ribbons are packed parallel to each other to form flexible fibrils which are oriented preferentially parallel to the fiber axis with long, thin pores between adjacent fibrils. No evidence for subgrain boundaries were observed by these authors, and the Moiré patterns found in the electron micrographs were interpreted as due to overlapping of the undulating ribbons. The intercalation of potassium vapor by PAN-based fibers (Ref. 29) does not destroy the fiber and has no effect on the preferred orientation of the ribbons, indicating that there is little crosslinking perpendicular to the layer planes and therefore no twist boundaries normal to the fiber axis, as suggested by Johnson and Tyson.[22] This simplified ribbon model for high-strength carbon fiber is shown schematically in Fig. 3.

A somewhat more complex but essentially similar model for PAN-based fiber, as proposed by Phillips, Hugo, and Roberts,[32] is illustrated in Fig. 4. Using lattice resolution transmission electron microscopy, no evidence of transverse subgrain boundaries was found in either PAN-based or rayon-based fiber samples, the packets of layer planes being continuous over long distances but with an occasional sudden or gradual curvature. A typical transmission micrograph of the periphery of a PAN-based Type I fiber is shown in Fig. 5. It is still quite possible that the absence of subgrain boundaries noted by these and other authors is a reflection of the exceptionally perfect regions of the fibers chosen for study. Clear examples of complex subgrain boundaries with twist and tilt components have been observed in boron-doped fibers[24] which contain crystallites of three-dimensional graphite of about 150Å thickness.

It is now well understood that the degree of preferred orientation of the structural units of the carbon fiber is very dependent on the final heat treatment temperature. Well-oriented arrangements, such as that shown in Fig. 5, are only found in those fibers which have been heat treated at temperatures above 2500°C. Fibers prepared at lower temperature (Type II) show only poorly developed crystallinity and preferred orientation. Figure 6 shows a transmission electron micrograph of a fiber of this type showing only isolated nuclei of oriented layer planes.

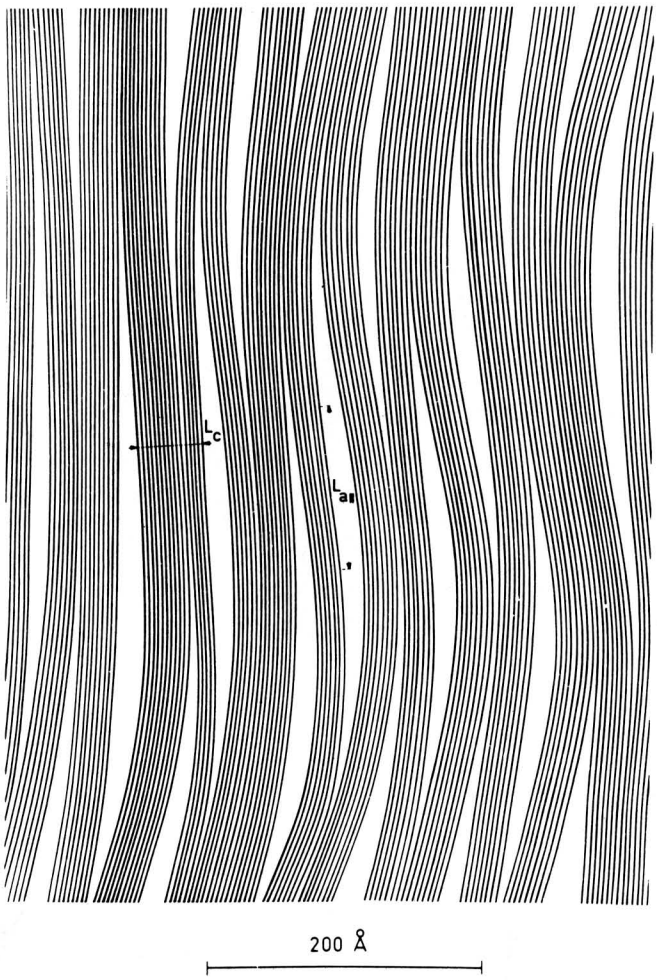

Fig. 3 Structure of high-strength carbon fiber, according to Ruland [from Perret and Ruland[29]].

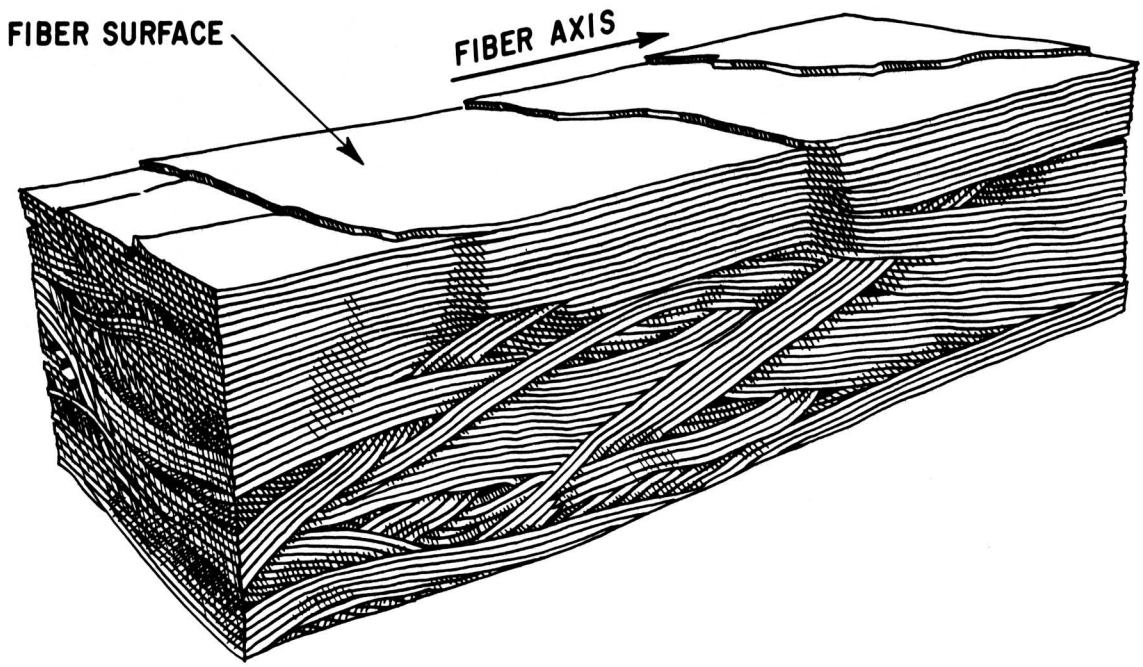

Fig. 4 Structure of high-strength carbon fiber, according to Phillips and Roberts [from Ref. 61, courtesy of B. W. Roberts, General Electric Company].

Fig. 5 Transmission micrograph of PAN-based Type I carbon fiber. (Courtesy of V. A. Phillips, General Electric Company.)

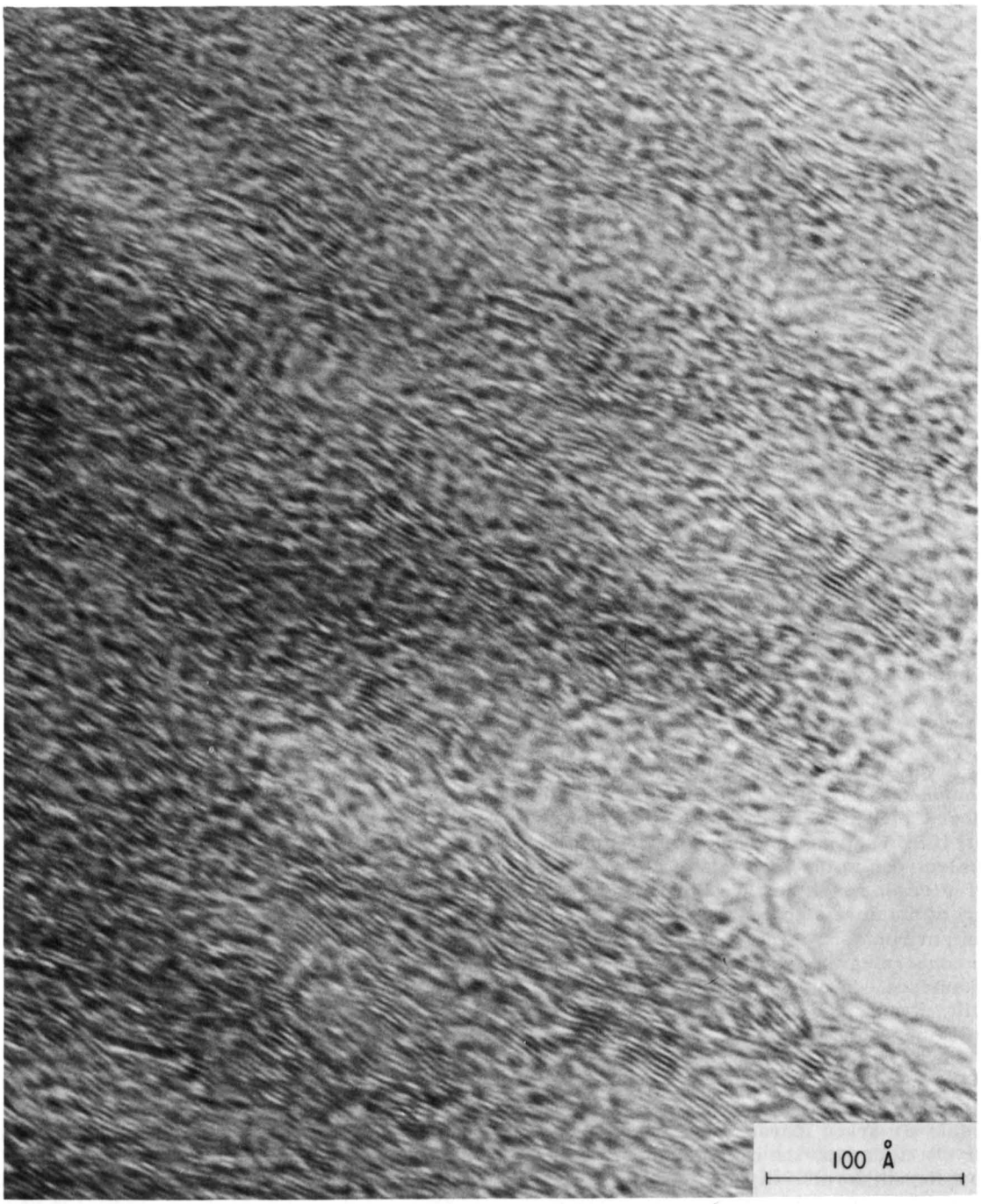

Fig. 6 Transmission micrograph of PAN-based Type II carbon fiber. (Courtesy of V. A. Phillips, General Electric Company.)

It is also interesting that even well-ordered fibers are themselves composite structures, with the core material having a distinctly different fine structure from the peripheral regions. Transverse sections of well-oriented fibers often show considerable curvature of the plane packets and a random arrangement about the fiber axis. Butler and Diefendorf,[33] using dark field electron microscopy, observed that rayon-based fibers had a randomly oriented interior but with a high orientation of the basal planes parallel to the fiber surface, whereas PAN-based fibers showed a more concentric structure. The more disorganized structure found in the fiber core appears to be the result of incomplete stabilization of the precursor fiber during processing. Thus Watt and Johnson[34] found that longer oxidation treatment of the PAN precursor increased the thickness of the well-oriented sheath and thereby improved the modulus of the fiber. Similarly, Johnson, Rose, and Scott[26] observed that the unstabilized core resulting from partial oxidation at 300°C before graphitization fused during heat treatment, giving rise to flaws and voids in the fiber interior. According to Jones and Duncan,[35-36] the decrease in modulus and tensile strength generally associated with increase in fiber diameter can be explained on the basis of different amounts of sheath and core regions in fibers of different diameters. The effect of structure on the mechanical properties of carbon fibers is discussed further in the following section.

Several novel spectroscopic techniques have recently been used to investigate the surface structure of carbon fibers. High-energy photoelectron spectroscopy (ESCA) gives a measure of the binding energies of electrons in the 1s levels of carbon, oxygen, and nitrogen in the surface layers. Shifts in the energy of the core electrons are sensitive to the chemical environment of the atoms and yield information concerning the functional groups present on the fiber surface. Typical results, obtained by Barber, Swift, Evans, and Thomas,[37] for a PAN-based Type II fiber which had been baked to 1000°C in nitrogen are shown in Fig. 7 (top spectra). The spectra for the same fiber following an oxidation treatment are also shown (bottom spectra). Comparison reveals a marked increase in surface-bound oxygen after the oxidation, the oxygen being held in at least two different forms. Appreciable amounts of nitrogen are also detectable on the fiber surface, although these can be almost completely removed by heating to 2000°C.

Trace amounts of surface impurities in carbon fibers have also been detected by Auger electron spectroscopy, which is particularly useful in identifying the elements present in the first few atomic layers of the surface. Results obtained by Connell[38] for a PAN-based Type II fiber are shown in Fig. 8, in which the derivative of the energy distribution $dN(E)/dE$ of the emitted electrons is plotted against the electron energy. Small concentrations of P, S, Cℓ, and O are in evidence.

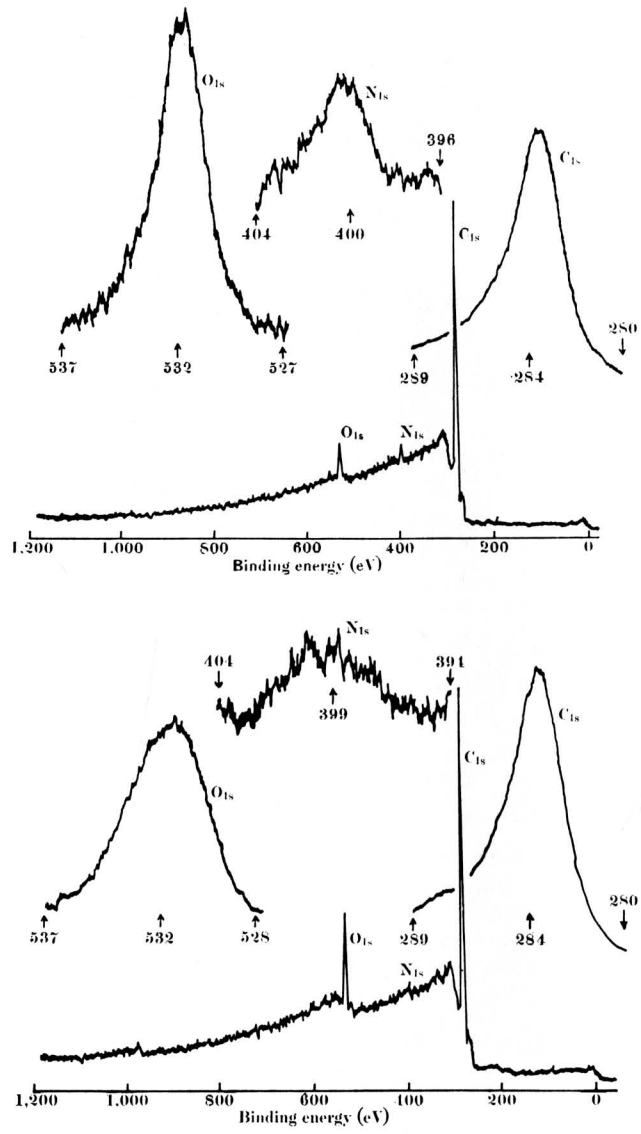

Fig. 7 High energy photoelectron spectra of 1s N, O, and C electrons in Type II carbon fiber. Top spectra--fiber baked in N_2 at 1000°C. Bottom spectra--fiber baked in N_2, then oxidized. [From Barber et al.[37]].

An ingenious method for investigating the crystalline structure of carbon fiber surfaces has recently been developed by application of laser-induced Raman spectroscopy, which can be used to distinguish between different types of carbon and graphite. Materials which are completely graphitic exhibit a single Raman peak at 1575 cm^{-1}, whereas less crystalline forms of carbon show a second peak at 1355 cm^{-1}. Raman spectra for PAN-based Types I and II fibers, obtained by Tuinstra and Koenig[39] are shown in Fig. 9. The differences in line width prove that the Type II fiber has essentially a carbon

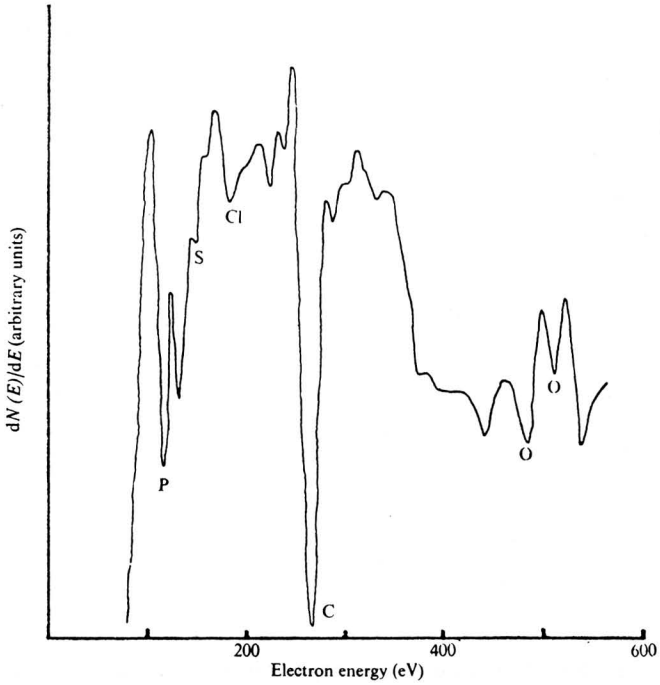

Fig. 8 Auger electron spectra of PAN-based Type II fiber [from Connell[38]].

surface, whereas the Type I material, heat treated to a higher temperature, is more graphitic with larger surface crystallites. This technique can also be used to estimate the apparent crystallite size and the relative amount of edge dislocations, crystal edges, and vacancies. A correlation between these features and composite shear strengths has been claimed. [40]

Mechanical Properties

For obvious technological reasons, much attention has been paid to the effects of heat treatment and applied stress on the degree of preferred orientation and crystallite size and the relation between these structural features and the mechanical properties of the fibers. Much effort has also been expended in identifying structural defects which may be the cause of failure and in estimates of the theoretical ultimate properties attainable with perfect structures.

By using neutron diffraction, Saunderson and Windsor[41] have studied the changes in orientation induced in PAN-based fibers as a result of heat treatment. The intrinsic width of the (002) Bragg reflection was used to measure the mean crystallite size along the graphite c-axis, L_c, whereas the variation of intensity of this reflection with the tilt angle of the fibers gave an estimate of the spread of orientation of the crystallite c-axes about the fiber axis, χ_c. L_c increased regularly with heat treatment temperature and varied directly with the modulus of the

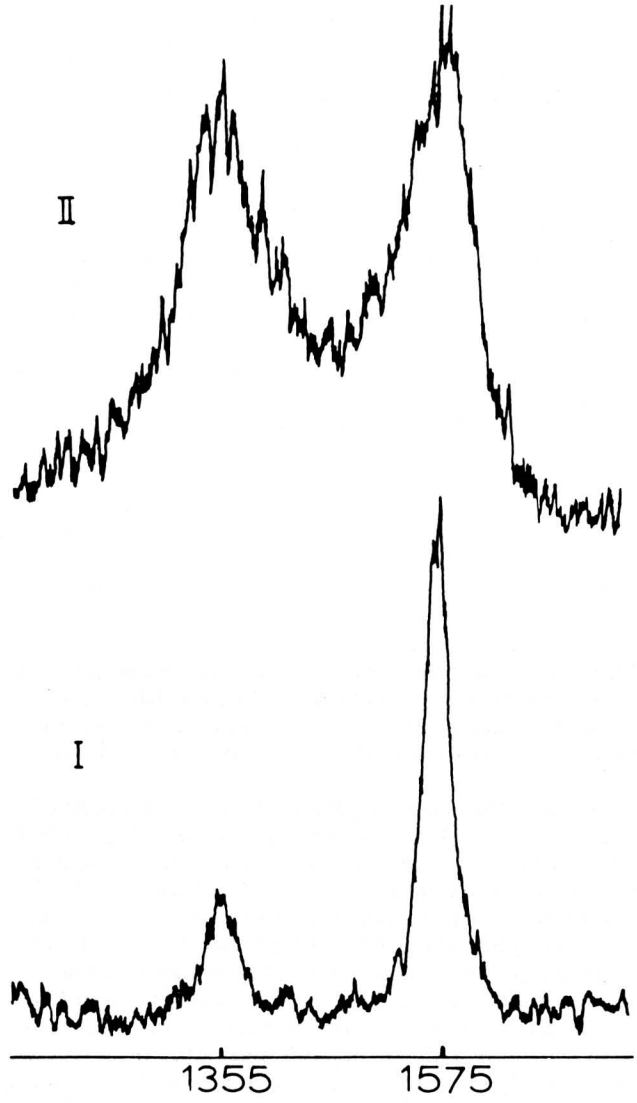

Fig. 9 Raman spectra of PAN-based Types I and II carbon fibers [from Tuinstra and Koenig[39]].

fibers. On the other hand, χ_c changed in a more complex manner with increasing temperature, being nearly constant up to 1500°C and then decreasing at higher temperatures. As the ultimate tensile strength also attained a maximum value at about 1500°C, [42] it seems likely that a common mechanism causes the decrease in fiber strength and the improvement in orientation above this point. The thermal activation energy which allows reorientation of the crystallites may also promote the migration of crystallographic faults and hence lead to the growth of macroscopic defects.

The oriented structures induced in high-strength carbon fibers by stress graphitization can also be partially destroyed by reheating the fibers to temperatures below 2000°C in the absence of an applied stress. [43] As expected, relaxation of the oriented

fibrillar structure of rayon-based fibers is accompanied by a marked reduction in mechanical properties. However, annealing to temperatures above 2400°C apparently induces additional graphitization and an improvement of 10% to 20% in modulus and fracture stress is found after heating to 2800°C.

The theoretical modulus of graphite single crystals is about 14 x 10^6 psi and the tensile strength with respect to the breaking of bonds in the layer plane is 26 x 10^6 psi, or about 18% of the modulus. Although graphite whiskers have tensile strengths as high as 3 x 10^6 psi, the strength of the best carbon fibers yet produced is less than 1% of the modulus. The reason for this low strength in carbon fibers has been discussed by several authors. Williams, Steffens, and Bacon[27] consider that the tensile strengths are dependent on flaws present in the fibers and, as the fracture appears to be intergranular, the strength is limited by the fibrillar microstructure and therefore cannot be expected to approach the theoretical values for single graphite crystals. In a similar vein, Reynolds[44] analyzed the elastic constants of carbon fibers as a function of crystallite alignment, and concludes that although more perfect fibers with better orientation and crystallite size would show increased shear and axial modulus, the transverse and torsional moduli would be reduced.

It has often been suggested that the strength of carbon fibers is limited by the presence of flaws both in the interior and on the fiber surfaces. Thus surface deposits are often observed in commercial PAN-based fibers, due probably to carbonization of droplets of the polymer precursor on the surface of the fibers during heat treatment. These can be selectively removed by etching in moist air,[45] leading to an increase in the tensile strength. Internal flaws consist of inorganic or organic particles or voids which result in a decrease in strength with increasing test gauge length[46] and with fiber diameter[36] even with samples that have been etched to remove surface defects. It can be estimated that the tensile strength of carbonized PAN-based fiber is in the neighborhood of 10^6 psi in the absence of bulk and surface flaws.[47] These fibers, when heat treated to 2800°C, show nonelastic effects with the modulus decreasing with increase in strain. This nonlinear behavior first becomes detectable in PAN-based fibers at heat treatment temperatures above 1600°C but appears to be general in rayon-based material.[27] On the basis of their undulating-ribbon model, Perret and Ruland (Ref. 48) consider that the deformation processes which occur with increasing strain rates are, initially, an irreversible unwrinkling of the ribbons followed by gliding of individual ribbons relative to each other at high strain rates. A similar failure mechanism, based on the shearing of the graphitic crystallites in the fibers, has recently been proposed by Cooper and Mayer.[42] As the applied stress is increased, glissile dislocations move towards the crystallite boundaries and build up there until the critical crack nucleation stress is reached, at which point failure will ensue. This explanation suggests that the strength of carbon fibers could be improved not only by reducing the incidence of flaws and voids, but also by decreasing the crystallite size and by eliminating dislocation motion as a result of hot stretching and solid solution hardening.

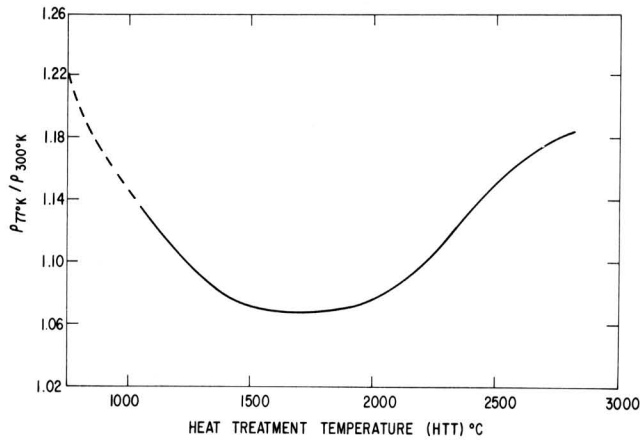

Fig. 10 Variation of resistivity ratio ρ_{77}/ρ_{300} of PAN-based carbon fiber with heat treatment temperature [after Robson et al. (50)].

Electrical and Electronic Properties

The evolution of structure in carbon fibers as a function of heat treatment can also be followed by measuring changes in electrical and electronic properties. The specific electrical resistivity of carbon fibers prepared from a number of precursors shows a steady decrease with increase in modulus.[49] Although this variation is obviously a reflection of the degree of preferred orientation of the crystallites along the fiber axis, even for the most highly oriented fibers the resistivity is still considerably larger than the basal plane resistivity for graphite single crystals (about 4 x 10^{-5} ohm cm at room temperature).

Robson, Assabghy, and Ingram[50] have carried out resistivity, thermoelectric power, and magnetoresistance measurements on PAN-based fibers heat treated at temperatures between 1000° and 2800°C. (HTT). In general, the longitudinal resistivity decreases with increasing HTT in this range and the resistivity measured between 77° and 500°K falls more or less linearily with increasing HTT. As shown in Fig. 10, the resistivity ratio ρ_{77}/ρ_{300} falls with increasing HTT up to about 1750°C and then increases again for HTT above 2000°C. For HTT below 1000°C, the resistivity shows the exponential variation with temperature typical of an intrinsic semiconductor. The negative temperature coefficient of ρ between 77° and 500°K is similar to that observed for pyrolytic graphite and is quite different from that of single-crystal graphite which shows a positive coefficient (Ref. 51).

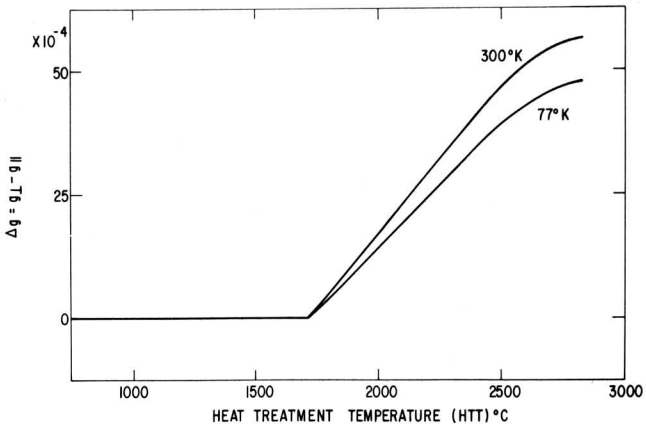

Fig. 11 Variation of g-value anisotropy for PAN-based fibers as a function of heat treatment temperature [after Robson et al. (52)].

Measurements of thermoelectric power also show that the Seebeck coefficient of carbon fibers changes sign at a HTT of 1750°C and becomes positive at higher temperatures. There are also indications that the transverse magnetoresistance changes sign from positive to negative at the same critical point. In addition, the HTT of 1750°C corresponds to abrupt changes in the ESR properties of PAN-based fibers (Ref. 52). As indicated in Fig. 11, the g-value anisotropy ($\Delta g = g_{\perp} - g_{||}$) at 77° and 300°K increases sharply as the HTT reaches 1750°C. Following the onset of this anisotropy, Δg increases with increasing HTT and reaches saturation above 2600°C, probably as a result of the crystallites attaining almost complete alignment of their basal planes parallel to the fiber axis. These results all lead to the conclusion that a major change in the electronic properties of the fibers occurs at a HTT in the neighborhood of 1750°C which is probably associated with a sudden increase in the degree of graphitization. Abrupt changes in mechanical properties should also occur in this region and indeed PAN-based fibers begin to exhibit nonelastic behavior after heat treatment to about 1800°C and, in addition, the modulus/rigidity ratio shows a discontinuity at this point. (47) As rayon-based fibers show non-Hookean behavior when prepared at lower HTT, it would be interesting to determine if this structural difference is reflected in the electronic and ESR properties of the two types of fibers.

Irradiation Effects

The effects of neutron irradiation on the physical properties of carbon fibers has received some recent attention. Allen, Cooper, and Mayer(42, 53) first reported that irradiation of PAN-based fibers to a dose of 2.2×10^{17} n cm^{-2} at pile temperature caused increases in Young's modulus and fiber strength but had little effect on resistivity. On the other hand, boron doping increased the modulus and decreased the resistivity whilst the fiber strength remained unchanged. It was suggested that irradiation, as with boron doping, hinders dislocation motion and thereby leads to increases in modulus by a "solid-solution hardening" process.

More detailed studies of the effects of irradiation on PAN-based fibers have been carried out by Bullock. (54) Type II fibers (HTT < 1500°C) after irradiation in air showed a sharp increase in tensile strength with a neutron fluence of 6×10^{17} n cm^{-2}, reaching a maximum value of 17% above that of the unirradiated fibers for a fluence of 8.5×10^{17} n cm^{-2}. With higher neutron exposure in air the strength decreased, apparently as a result of oxidative degradation. In liquid nitrogen the strength of these fibers continued to increase with neutron dose and was about 30% greater than that of the original fibers for a fluence of 3×10^{18} n cm^{-2}. On the other hand, Type I fibers (HTT > 2000°C) showed only a slight increase in strength on irradiation in air and a small decrease on irradiation in liquid nitrogen. A significant increase in susceptibility to air oxidation was also found by Murphy and Jones(55) following irradiation of PAN-base fibers, an effect which was attributed by the authors to radiation damage induced in surface flaws.

Irradiation at elevated temperatures can also lead to a degradation of the fibers. Jones and Peggs(56, 57) found that both the modulus and fracture strength of PAN-based, high modulus (Type I) graphitized fiber decreased by about 20% on irradiation at 420°C to a fluence of 4.8×10^{20} n cm^{-2}. Under these conditions the radiation induced flaws and cracks in the fiber structure, the incidence of which rose as the temperature during irradiation increased from 420° to 500°C. Experiments with a lower modulus fiber (Type II) showed an increase in both fracture strength and modulus following irradiation at 550°C to a fluence of 6.6×10^{20} n cm^{-2}, which appeared to be associated with an increase in apparent crystallite size. (58) Evidently low and high modulus fibers are different in their response to radiation, and a qualitative attempt to explain this difference in terms of the sheath and core structure has been made by Bullock. (59) In summary, on the basis of the available evidence, it does not appear likely that the mechanical properties of carbon fibers can be dramatically enhanced by means of a radiation treatment.

Porosity and Surface Area

The porous structure of high-strength carbon fibers is dependent on the nature of the precursor and on the heat treatment history of the material. As noted above, various types of pores have been identified in PAN and rayon-based fibers, particularly voids, bubbles and flaws, and also lenticular cavities between fibrils. Most of this porosity is locked into the fiber interior and is therefore not accessible to

gas adsorption. Internal voids may, however, play an important role in determining fiber strength and modulus. (60)

The results of early measurements of fiber porosity and surface area have been described in a recent review. (61) PAN-based fibers generally show lower surface areas (0.1 to 0.4 $m^2 g^{-1}$) than those derived from rayon (0.5 to 1.5 $m^2 g^{-1}$). This difference is consistent with the surface morphology of the two types, those derived from PAN having smoother exterior surfaces than those obtained from cellulosic precursors. Recently, Spencer et al. (62) carried out displacement density and adsorption measurements on carbon fibers at various stages of preparation from PAN. Porosity accessible to helium but not to a silicone liquid increased from about 1% for the raw PAN polymer to over 15% following heat treatment to 1000°C, and then decreased rapidly at higher temperatures, whereas sorption of krypton reached a maximum following 600°C heat treatment. At temperatures above this, progressive closure of the surface pores took place so that the krypton sorption was reduced.

Further evidence for an internal pore system in PAN-based fibers has been obtained by Byrne and Jeffries, (63) who measured the surface areas and helium densities of the fibers before and after grinding to a fine powder. Grinding produces a very large increase in nitrogen adsorption and also a marked increase in helium density, indicating that an internal system of pores has become open to gas penetration. That some of the existing pores may be filled with incompletely carbonized material is indicated by the results of Mimeault and McKee (64) who found regular increases in krypton surface areas of PAN-based fibers as the outgassing temperature was raised progressively from 100° to 1000°C. This increase in area was accompanied by the evolution of a complex mixture of oxides of carbon and nitrogen, water, methane, hydrogen, and small amounts of C_3 and C_4 hydrocarbons. The concentration of hydrocarbons in the desorbed gas decreased with increasing temperature, and above 500°C only CO, CO_2, and H_2 evolved. The highest surface area observed was of the order of 1 $m^2 g^{-1}$ (following outgassing at 1000°C), whereas ground fibers of the same type gave surface areas exceeding 100 $m^2 g^{-1}$.

The surface area of carbon fibers also depends to a large extent on the nature of the precursor polymer and on the chemistry of the pyrolysis reaction. Whereas fibers derived from rayon and PAN show low surface areas after heat treatment, fibers prepared by the decomposition of Saran, which evolves large quantities of gas on pyrolysis, are highly porous with surface areas approaching 1000 $m^2 g^{-1}$. (21) A similar porosity is found in carbon fibers derived from polyacetylene following carbonization at 1000°C. (65)

Surface Reactivity

The surface properties of carbon fibers are of considerable practical importance in determining the extent to which the fibers can bond to organic matrix materials and thereby produce strong composite structures. Much effort has been devoted to changing the surface condition of the fibers, and hence improving such composite properties as interlaminar shear and compressive strength. Earlier work in this area has been the subject of a recent review. (61)

Most of the successful surface treatments used in the past have involved a partial oxidation of the fibers with a gaseous or aqueous reagent. Oxidation in air or in other gas mixtures containing oxygen was much used in the earlier work; and although substantial improvements in composite properties were obtained in many cases, the process proved difficult to control as oxidative etching is often nonuniform and excessive reaction produces marked pitting of the fiber surface and reduced tensile strength. Pitting during oxidation can be reduced, however, by adding an oxidation inhibitor, such as a halogen or halogenated hydrocarbon, to the oxygen-containing atmosphere. (66) Another approach is to catalyze the oxidation at lower temperature by treatment of the fibers with a solution of a catalytic additive, such as a copper salt. (67) Copper catalyzes the oxidation of graphite with formation of channels in the basal plane, rather than etch pits along the c-axis. (68) Recently, wet oxidation processes have become more popular, and several oxidizing solutions, such as nitric acid (69) and sodium hypochlorite (70) have been used to improve composite properties. Other effective treatments include coating the fibers with a solid oxidant such as potassium nitrate or permanganate, followed by heating in an inert atmosphere; (71) coating with an epoxy silane (72) and oxidation in reduced pressures of oxygen in a r-f discharge. (73) Considerable increases in composite shear properties have also been reported following treatment of the fibers with an organic resin and subsequent pyrolysis to cover the polymer with a carbonaceous coating. (40) This method increases the strength of the bond between fiber and matrix without the fiber degradation which often accompanies oxidative treatments.

The mechanism by which the fiber-matrix bonding is improved following surface treatment of the fibers is not entirely clear. In general, the composite shear properties decrease as the surface structure of the fibers becomes more highly graphitized. As chemical oxidants are known to introduce polar groups to unsaturated sites on the edges of the graphite basal planes, it is feasible that the improvement in composite shear properties results from chemical bonding between resin matrix and functional groups introduced to the fiber surface. The proportion of graphite basal plane present in the

fiber surface increases with fiber modulus, so it is plausible that the higher shear strengths found with lower modulus fibers are a reflection of the greater chemical bonding of the matrix to edge carbon atoms present in the fiber surface. On the other hand, pre-oxidized fibers often retain their improved shear properties even after heating in vacuum to temperatures as high as 900°C, [74] under which conditions functional surface groups would certainly be completely removed. A correlation between specific surface area and shear strength is reported by Scola and Brooks[70] for rayon-based fibers, but no such relation exists for PAN-based fibers. [74] However, because increases in surface area generally result from the formation of pores in the 6Å to 30Å range, it is unlikely that this microporosity will affect the adsorption of the large resin molecules of the matrix polymer. It is possible also that etching effectively removes surface deposits and flaws which can act as stress-risers, causing failure to occur at less than optimum values with untreated fibers. [47] An overall smoothing of the surface topography of PAN-based fibers following oxidation by CO_2[75] and nitric acid[74] is generally found.

Adsorption measurements can also be employed to investigate the changes induced in fiber surfaces by oxidation. Untreated carbon fibers give heats of adsorption of organic vapors similar to those for graphitized carbon black, and little change occurs on treatment of the fibers with nitric acid. [76] However, nitric acid treatment results in a marked increase in the initial adsorption coefficients of many adsorbates (Ref. 77). Recently, Scola, Golden, and Brooks, [78] by measuring the adsorption of Li^+ ion from solution showed that nitric acid treatment creates acidic sites on the fiber surface, an effect which is not observed following etching with oxygen. Clearly more work must be carried out in this area before the nature of chemical activation treatment is completely understood.

Metal-coated Carbon Fibers

The possibility of reinforcing metals with high-strength carbon fibers to improve creep resistance, toughness, and elastic moduli has stimulated many investigations of carbon fiber-metal compatibility. Most refractory metals, such as Ti, Cr, and Mo, are unsuitable as they form stable carbides which diminish the strength of the fibers, whereas carbon is soluble to some extent in Ni and Co at elevated temperatures. Nevertheless, several studies have been made of the effect of these and other metal coatings on the mechanical properties of carbon fibers.

Early work by Jackson and Marjoram[79] demonstrated that heat treatment of Ni and Co-coated fibers at 1100°C caused recrystallization of the fibers to three-dimensional graphite, accompanied by a drastic decrease in fiber strength. More recently, [80] the same authors have studied single fibers electroplated with Ni and Co and then heat treated for varying periods in vacuum at temperatures up to 1100°C. A marked loss in strength of Ni-coated carbonized fiber was noticed after heating for one day at 700°C, and after one day at 1000°C, with graphitized fibers coated with Ni and Co. This decrease in strength correlated with a progressive increase in crystallite size and a decrease in the mean interlaminar spacing. Three-dimensional (101) and (112) diffraction lines appeared during this growth process, the pattern finally becoming identical with that natural graphite. The metal is apparently acting as a catalyst for the graphitization process, which involves dissolution of carbon in the metal layer, followed by reprecipitation in a more fully crystalline form. Fiber recrystallization is also accompanied by a migration of Ni towards the fiber interior.

Similar results have been obtained by Barclay and Bonfield[81] with PAN-based fibers coated with an evaporated film of Ni. Marked reduction in fracture strength was again found after heating the coated fibers at 1080°C for 24 hours. However, these authors found no x-ray evidence for recrystallization of the fiber, which they attribute to the effect of impurities in the electroplated Ni used by Jackson and Marjoram. The loss in strength may be caused by dissolution of carbon in the Ni coating as, in the absence of heat treatment, Ni coatings do not cause fiber degradation. Thus the modulus of fibers electroplated with Ni obey a simple law-of-mixtures relation, the elastic metal coating yielding plastically before fracture of the fiber occurs. [82] However, a recrystallization of the Ni was observed on heating for 1 to 2 hours at 600°C, together with a slight drop in fiber modulus.

The degradation observed with Ni-coated fibers at elevated temperature is thus a serious limitation to the use of Ni as a matrix material in composites. Even though loss of strength does not occur below 600°C, temperatures in excess of this are generally used to fabricate composites by hot pressing. In addition, the Ni coating does little to improve the oxidation resistance of the fiber. Braddick, Jackson, and Walker[83] found complete loss of carbon from a Ni-carbon fiber composite on heating for 5 hours in air at 600°C, and there was some indication that the presence of Ni actually accelerated the oxidation of the fiber. This is not surprising in view of the known tendency of nickel oxide to catalyze the oxidation of graphite, [84] although a coherent coating of the metal may slow down the rate of oxidation of the fiber by limiting the diffusion of oxygen to the metal-carbon interface. [85]

Because of the poor thermal stability and oxidation resistance of Ni-(and Co) coated carbon fibers, more attention has recently been given to aluminum as a matrix material. Aℓ appears to be compatible with carbon fibers for long periods at temperatures up to 600°C and protects the fibers from oxidation. Various methods for electroplating Aℓ onto carbon fibers have been described. [86] The carbide $Aℓ_4C_3$ is formed at elevated temperatures, and this results in loss of tensile properties of Aℓ-coated fibers

heated to 1100°C. A promising way around this difficulty is to coat the fibers first with Ni and then with Aℓ by passage through a liquid metal bath. (87) The compound $A\ell_3Ni$ is apparently formed at the interface and promotes wetting of the fibers by the melt.

In summary, it may be said that because of the limited number of suitable metals and the cost and complexity of coating processes, metal matrix-carbon fiber composites are not as attractive today as they were two years ago. However, there is still the possibility of major breakthroughs in this area.

GLASS-LIKE CARBONS

It has been known for many years that certain thermosetting polymers pyrolyze to form disordered nongraphitizing carbons with glass-like properties. However, because of the large volume of gaseous decomposition products which were evolved during the reaction, these carbons were generally quite porous. About ten years ago a new type of synthetic carbon became available which was remarkable for its very low gas permeability, glass-like isotropic properties, high temperature stability and chemical inertness. Although details of the preparation procedures are not generally available for these materials, the low porosity can apparently be achieved by slow carbonization of the precursor resin under carefully controlled conditions in the solid state. The pores which are formed in the structure during gas evolution collapse on subsequent high-temperature treatment to leave a homogeneous vitreous residue whose unique properties suggest a number of novel applications.

Glass-like carbons are now produced commercially under a variety of trade names by Japanese, French, British, and U. S. manufacturers. Typical physical properties are listed in Table I. Although these materials have many common characteristics, the properties are to some extent dependent on the nature of the precursor polymer and on the details of the pyrolysis process. In addition, many fundamental investigations have been carried out with glass-like carbons prepared in the laboratory under a variety of conditions. For convenience of classification all these materials will be referred to as "glass-like carbons" with the understanding that this term may cover a spectrum of behavior.

TABLE I

Typical Physical Properties of Glass-like Carbons

Bulk density	1.3 - 1.55 g cm^{-2}
Apparent porosity	0 - 12%
Gas permeability	10^{-6} - 10^{-12} cm^2 sec^{-1}
Flexural strength	500 - 8000 kg cm^{-2}
Tensile strength	400 - 1000 kg cm^{-2}
Young's modulus	1400 - 3300 kg mm^{-2}
Thermal expansion coefficient	(2 - 3.5) x 10^{-6} deg. C^{-1}
Thermal conductivity	0.01 - 0.06 cal. cm^{-1} sec^{-1} deg. C^{-1}
Electrical resistivity	(10 - 50) x 10^{-4} ohm-cm
Shore hardness	70 - 125

Preparation and Chemistry

The formation of an impermeable glass-like material involves the slow carbonization of non-melting crosslinked polymers, with or without applied pressure. In determining the morphology of the product the chemical nature of the precursor is rather less important than the conditions of pyrolysis, and similar products can be prepared from a variety of starting materials. Thus "Vitreous Carbon" is prepared from phenolformaldehyde resin, "Vitrocarbon" from an acetone-furfural resin, and "Glassy Carbon" from polyfurfuryl alcohol or phenolic precursors. Other starting materials have included naphthalenediol, cellulose, cumarone, indene, cyclopentadiene, and pitch.

The complex chemistry of pyrolysis and the mechanism of conversion of organic resins to glass-like carbons has recently been reviewed by Fitzer et al.(88) The pyrolysis of polyfurfuryl alcohol, a typical precursor material, involves a volume shrinkage of about 50% between 200° and 800°C, while the bulk density increases from about 1.3 to 1.55 g ml^{-1}. The gaseous decomposition products, in addition to water, are methane (from elimination of methylene bridges), CO_2 and CO (from rupture of the furan rings). Above 500°C, hydrogen is evolved and carbonyl groups are eliminated to form a disordered crosslinked aromatic network which continues to shrink with increasing temperatures up to 1000°C with collapse of the pores formed by the previous gas evolution. The degree of crosslinking in the starting polymer does not appear to influence the microporosity and mechanical properties of the glass-like carbon residue, although the rate at which the gaseous products are eliminated certainly determines the residual porosity at various stages of the carbonization process.

Porosity and Surface Area

In the preparation of glassy carbon, from polyfurfuryl alcohol or phenolic polymers, pores in the 2μ to 20μ size range develop on pyrolysis to temperatures of 1000°C. (89) No pores can be observed in the optical microscope for samples treated to 500°C although porosity develops rapidly at higher temperatures, reaches a maximum at 800°C, and then diminishes again at still higher temperatures. As

expected, the maximum surface area and water adsorption capacity are also found for samples treated to 800°C.

Glass-like carbons prepared in the laboratory by Fitzer, Schaefer, and Yamada[90] from the same precursors showed quite different behavior. In this case no porosity could be observed optically at any stage of carbonization and even in the electron microscope no pores larger than 100Å (the limit of resolution) could be detected. Using x-ray scattering the mean pore radius was estimated to be 25Å, for samples heat treated to 3000°C. Because of this small pore size, adsorption of nitrogen at -195°C was very slow, although the BET surface area was higher than with the commercial "Glassy Carbon" samples. With the laboratory samples, micropore volume, surface area, and water adsorption all reached maxima for samples treated to 700°C. It is curious that the large volumes of pyrolysis products are able to escape without rupturing the solid matrix, and Fitzer has suggested that water escapes by a liquid transport process. By carbonizing polyfurfuryl alcohol resins in vacuum, Marsh and Wynne-Jones[91] obtained glass-like carbons with surface areas exceeding 400 $m^2\ g^{-1}$, although again the maximum values were found at carbonization temperatures in the 600° to 800°C range. Owing to a molecular sieve effect in the small pores, the surface area as determined by nitrogen adsorption at 77°K was considerably lower than that obtained using CO_2 at 195°K, and it is likely that these nitrogen adsorption data do not represent thermodynamic equilibrium values. This result should be borne in mind when considering the surface area values reported by Fitzer[90] and others.[92]

The shape-selective adsorption properties of glass-like carbons prepared from polyvinyl alcohol have also been noted by Schmitt and Walker,[93] the apparent surface area being appreciably lower when measured with iso-butane than with n-butane as adsorbate. Apparently a proportion of the pores are in the 5Å size range and thus are not accessible to the branched chain hydrocarbon molecules.

Structure

Although the detailed mechanisms of formation of glass-like carbons are evidently rather complicated and show many obscure aspects, the general features of their structure have now been clarified. Noda and Inagaki,[94] using x-ray diffraction, analyzed the first peak of the radial distribution curve for a series of glass-like carbons prepared at temperatures between 500° and 3000°C. The diffraction patterns remained diffuse even after the 3000°C treatment and resembled that of a small particle size carbon black. The interlaminar spacing decreased and the crystallite size increased with rising temperatures, although the degree of crystallinity was much lower than that of a petroleum coke heated to the same temperature. Analysis of the radial distribution curve indicated that two types of C atom were present, having respectively tetrahedral (sp^3) and trigonal (sp^2) coordination. It was plausibly suggested that small two-dimensional domains of graphitic planes are linked in an irregular manner by tetrahedral C atoms. With increasing temperature the proportion of trigonally bonded domains increases, so that the (002) diffraction line becomes sharper.

A somewhat different model was proposed by Kakinoki,[95] who suggested that domains of tetrahedral and trigonally bonded C atoms were linked by oxygen bridges. However, the oxygen content of most glass-like carbons is not sufficient to support this structure. A further model which does not assume the existence of trigonally bonded graphitic domains has been suggested by Furukawa,[96] who explains the isotropic physical and chemical properties of glass-like carbon on the basis of an irregular three-dimensional network of tetrahedral, double, and triple bonds. However, the presence of tetrahedral bonds between ordered domains and the existence of a separate highly disordered phase has been disputed by Ruland.[97] Experimental values for the heat capacity of glass-like carbon between 5° and 350°K show a T^2 dependence as with pyrolytic graphite,[98] suggesting that a two-dimensional layer lattice is present. In addition, tetrahedral C atoms are normally unstable at temperatures well below the firing temperature of glass-like carbons.

Direct analogies between the structure of glass-like carbon and carbon fibers have recently been revealed by high resolution phase-contrast microscopy. Electron micrographs obtained by Jenkins and Kawamura,[99] Phillips,[100] and by Ban and Hess[101] indicate that glass-like carbon is composed of tangled bundles of long microfibrils which show the 3.4Å basal plane spacing of graphite at high resolution. As shown in Fig. 12, packets of 2 to 10 planes maintain continuity over long distances, although changes in direction are found about every 50Å. These dimensions are in general agreement with the values of 15Å to 50Å estimated for the "crystallite size" in Vitreous Carbon by Cowlard and Lewis on the basis of x-ray line broadening.[102] From the results of a detailed study of the structure of glass-like carbon prepared by pyrolysis of a phenolic resin, Jenkins, Kawamura, and Ban[103] conclude that both glass-like carbon and high-strength carbon fibers possess a similar microfibrillar structure, the only essential difference being in the degree of preferred orientation induced in the graphitic ribbons during processing. Figure 13 shows a schematic model for the network structure of glass-like carbon as proposed by these authors. It is probable that closed micropores are present in this structure, thereby accounting for the low observed density, but the fibril bundles are certainly more tightly packed than suggested by Fig. 13.

Mechanical Properties

In common with other forms of carbon, the tensile strength of glass-like carbon generally increases

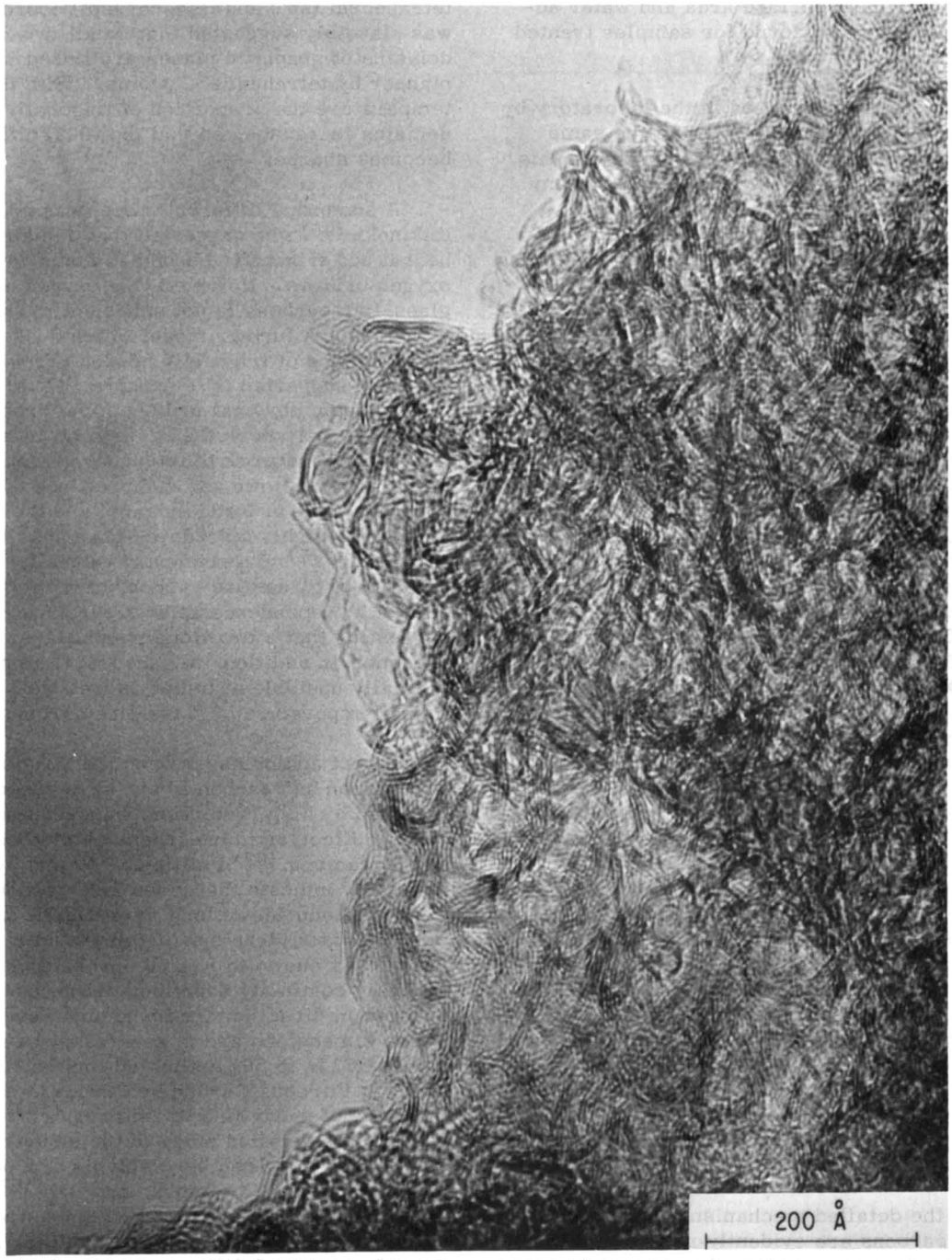

Fig. 12 Transmission electron micrograph of glass-like carbon. (Courtesy of V. A. Phillips, General Electric Company.)

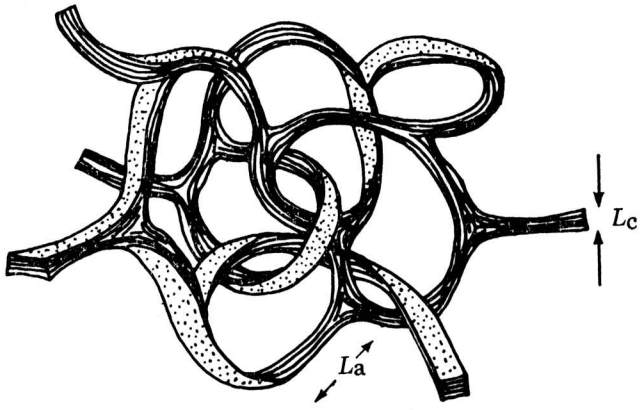

Fig. 13 Structure of glass-like carbon, according to Jenkins, Kawamura and Ban (from Ref. 103).

with temperature up to about 2500°C, whereas the elongation between 2500° and 2700°C is larger than for other graphitic materials. In addition, the Young's modulus of glass-like carbon reaches a maximum value following heat treatment to 1800°C (Ref. 104).

Internal friction measurements on glass-like carbons have been reported by Tsuzuku[105] and, more recently, by Taylor and Kline,[106] with some minor differences between the various materials used. Tsuzuku's earlier work with a Glassy Carbon sample revealed maxima in internal friction at 135°, 165°, and 200°K, respectively, whereas a later sample showed only a slight peak at 155°K. The internal friction values reported by Taylor and Kline for Vitreous Carbon were essentially independent of temperature up to 400°K, but with a small inflection in the dynamic elastic modulus at 50°K which may have been due to the presence of impurity. This behavior differs from that of graphite, which generally shows one or more internal friction peaks over this temperature range. These peaks are believed to be due to motion of dislocations associated with the crystallites. In the case of glass-like carbon, crystallites apparently play only a minor role in relaxation behavior.

Recently, the tensile creep behavior of glass-like carbon has been determined by Fischbach[107] over the stress range 500 to 18,000 psi and for temperatures in the range 2500° to 2900°C. For two grades of glass-like carbon the high-temperature deformation occurred at nearly constant volume with the high activation energy of 350 kcal mole^{-1}. Glass-like carbon also shows progressive creep hardening and a large creep recovery on removing the stress at high temperature. This behavior appears to be significantly different from that of graphitizing carbons and graphite.

Electrical Properties

As a consequence of the disordered structure, the electrical resistivity of glass-like carbon is generally considerably larger than that of more crystalline forms. However, the resistivity of the former decreases sharply with high temperatures and approaches that of soft carbon following heat treatment to 3000°C. From measurements of the change in resistivity with temperature, the energy gap between filled and conduction bands in Glassy Carbon has been estimated as 10^{-2} to 10^{-3} eV.[108] Measurements of changes in Hall coefficient, thermoelectric power,[108] magnetoresistance,[109] and magnetic susceptibility[110] as functions of heat treatment have also been made with glass-like carbons. Irradiation with neutrons showed much less change in the electrical and thermal properties than with graphite, although the contraction induced by the radiation was much greater than that reported for nuclear graphite.[111]

Reactivity

Glass-like carbons usually show much lower chemical reactivities than more highly ordered pyrolytic carbons and graphite. This relative inertness is associated with the low permeability and surface area, and therefore is dependent on the conditions of preparation. For this reason, and also because the impurity level is extremely variable, reported gasification rates of glass-like carbons vary widely among different investigators.

Cowlard and Lewis[102] report that Vitreous Carbon had the lowest rates of oxidation in dry air of a number of carbon samples of varying crystallinity, although impurities in the form of metallic oxides had a marked influence on the kinetics. The oxidation rate of glass-like carbons has been found to reach a maximum value at about 1100°C, and it is possible that a progressive deactivation of the active centers occurs at higher temperatures. It is also certain that catalytic impurities are important factors in determining the sites for oxygen attack on the carbon substrate. Thus Marsh and Rand[112] showed that preferential gasification by CO_2 took place in the vicinity of Fe and Ni impurities deliberately added to a porous polyfurfuryl alcohol carbon before carbonization. These metallic inclusions agglomerate during high-temperature treatment and eventually become inactive by conversion to oxide. The pitting observed on oxidation of Vitreous Carbon[113] is also certainly related to the presence of metallic impurities near the surface.

Glass-like carbon also shows considerable inertness towards oxidizing solutions that readily attack graphite. For example, Lewis, Redfern, and Cowlard[114] found a weight loss of only 0.5% for Vitreous Carbon after treatment for 6 hours at 120°C with a 1:4 mixture of nitric and sulfuric acids, whereas graphite is attacked rapidly at room temperature

with this reagent. Similarly, Glassy Carbon showed no change after 150 days' immersion in a 1:1 nitric-sulfuric acid mixture at room temperature. (104)

In view of the disordered structure of glass-like carbon, the formation of intercalation compounds would appear to be unlikely. However, reaction does occur vigorously with potassium vapor, leading to explosive shattering of the structure at 400°C(115) with some degree of intercalation. Glass-like carbon is also attacked by fused alkalis and by metal oxides, such as those of lead and barium, which are known to be powerful oxidation catalysts for carbonaceous materials. In these environments, glass-like carbon does not appear to be superior to other forms of carbon, although a relative inertness to molten metal halides and tellurium compounds has been claimed. (102) Thin layers of carbides are formed when glass-like carbon is heated with Si, Zr, and Nb, whereas metals such as Ni, Co, Fe, Pt, and B promote graphitization at temperatures above 1500°C. (116)

Graphitization

Glass-like carbons are very resistant to graphitization and, in the pure state, can be heated to temperatures in excess of 2000°C for long periods without appreciable crystallization. In some cases a partially graphitized skin has been observed to form after heating in an inert gas at temperatures of 3000°K. (117) A comprehensive review of the kinetics and mechanism of the graphitization process in various types of carbon has recently appeared. (118) The process is accelerated at high pressure. Following treatment at progressively higher temperatures under a pressure of 10 kbar, Glassy Carbon graphitizes in three stages, (119) the $\bar{d}$ value dropping in steps to 3.43Å at 1000°C, then to 3.38Å at 1800°C, and finally to 3.36Å at temperatures exceeding 2600°C. At 1 atm pressure only the first stage is observed.

The graphitization of glass-like carbon is strongly catalyzed by a number of metals and metallic carbides, although as with other catalytic processes, there is considerable discrepancy between results reported by different investigators. Glass-like carbons prepared from polyfurfuryl alcohol have been found to graphitize at temperatures as low as 1500°C in the presence of CuO and Aℓ, (120) whereas molten Cu metal is inactive. Glass-like carbon is strongly attacked by molten carbides of V, Ti, and Zr, resulting in recrystallization to well-ordered graphite (Ref. 121). More recently, three types of behavior have been observed on melting metals in glass-like carbon crucibles: (116)

(i) Rapid diffusion of metal into the crucible and conversion to graphite -- found with Ni, Co, Fe, Pt, Mo, Cr, and B.

(ii) Thin layers of a carbide phase formed at the interface between carbon and metal, but no graphitization -- found with Si, Zr, and Nb.

(iii) No catalytic graphitization -- Ag, Mg, Zn, Cd, Ge, Sn, Pb, Cu, Aℓ, Sb, Bi, Se, Te, and Pd.

Catalytic graphitization occurs by a solution-precipitation mechanism the driving force for which, according to Fitzer and Kegal, (121) is a difference in free enthalpy between disordered carbon and well-ordered graphite; this results in a higher equilibrium solubility of disordered carbon than crystalline graphite in a molten carbide phase (e. g. , VC). Thus the carbide droplet, when saturated with respect to the disordered carbon, will be supersaturated with respect to graphite which continuously precipitates as the droplet migrates through the glass-like carbon matrix. Gillot(122) has suggested that a similar process may occur even when the metal or carbide phase is not molten. In this case the solid particles can migrate through the disordered carbon mass leaving trails of crystalline graphite in their wake. However, the migration of solid particles through the matrix is likely to be much slower than the penetration of liquid droplets and the inactivity of Si, Nb, and Zr as graphitization catalysts is probably a reflection of the high melting points of the carbides of these metals. Nevertheless, in view of the wide range of stability of the carbides of the known metallic graphitization catalysts, it seems unlikely that a single mechanism is responsible for all the observed effects.

NEW ALLOTROPES OF CARBON

White Graphite

In 1968, a new allotropic form of carbon was identified in shock-fused graphite gneisses from the Ries Crater in Bavaria. (123) The new phase, which showed a reflection color of grey-white, was slightly harder and more reflecting than graphite. The x-ray pattern corresponded to a primitive hexagonal cell with dimensions $a_0 = 8.948Å \pm 0.009Å$, $c_0 = 14.078Å \pm 0.017Å$, and no (0001) reflections were observed. The calculated density was 3.43 g cm^{-3}, giving 168 atoms per cell. Subsequently the name "chaoite" was proposed for this new carbon modification.

Although only very small amounts of this natural material have been isolated, it has recently been claimed that an identical white form of carbon is produced at high temperatures and low pressure during graphite sublimation. (124) On heating small bars of pyrolytic graphite at temperatures of 2700° to 3000°K in 10^{-4} torr or argon, a silvery white coating was observed to form in the region of maximum temperature. Microprobe analysis showed this material to be carbon with up to 2.5% of Si impurity. Electron diffraction apparently confirmed that the deposit was composed of single crystals of hexagonal symmetry, the measured $\bar{d}$ values corresponding closely with the published values for natural chaoite. More recently the same authors

have reported the formation of white deposits when a number of different carbons are irradiated with a CO_2 laser[125], the material being identified as chaoite by means of ion microprobe mass analysis.[126] In spite of these seemingly definitive reports from one laboratory, several other groups have tried unsuccessfully to reproduce these experiments.[127] Independent confirmatory work is obviously needed in this area and at the present time "white graphite" appears to be the carbon analog of "polywater."

Linear Carbon Polymers

An interesting linear allotrope of carbon, in which the C atoms are arranged as a chain polymer with sp-hybridization, has been synthesized by Sladkov et al.[128] Polydehydrocondensation of acetylene in the presence of salts of bivalent Cu gave an unstable mixture of $H(C{:}C)_nH$ and Cu polyacetylenides. This product was freed from copper by oxidation with aqueous iron perchlorate, followed by extraction with aqueous ammonia and then hydrochloric acid. Final heat treatment was carried out under vacuum at 600° to 1000°C. The residue proved to be a stable black crystalline polymer of carbon, christened "carbyne" by the authors and containing the two linear modifications, polyyne $(\cdot C{:}C\cdot C{:}C\cdot)_n$ and polycumulene $(:C:C:C:C:)_n$. The hexagonal unit cell of the polyyne structure (a=b=5.09Å, c=7.80Å) contains 18 C atoms, the chains running parallel to the c-axis, whereas the polycumulene cell (a=b=4.76Å, c=2.58Å) has six C atoms, arranged in pairs. The calculated densities of these two forms are 1.97 and 2.25, respectively. The carbyne polymer proves to be extremely inert chemically and is resistant to attack by halogens and hydrogen. Prolonged reaction with ozone converts the polyyne structure to oxalic acid and the cumulene component to CO_2. The thermodynamic stability of carbyne appears to be greater than that of diamond and graphite at room temperature as a result of the conjugation energy of the π-electrons associated with the carbon chains.

MICROSCOPIC STUDIES OF GRAPHITE GASIFICATION

Space limitations do not permit a discussion of the complex field of carbon gasification kinetics, an area which has been reviewed thoroughly at regular intervals, especially by Walker, Shelef, and Anderson[129] and, more recently, by Lewis.[130] Instead, this final section will be devoted to a brief summary of a few recent investigations of the reactivity of graphite single crystals, as determined by microscopic methods. Graphite crystals are very amenable to optical and electron microscopic study, as carbon gasification reactions are among the few types of gas-solid reactions which yield only gaseous products. In addition, natural graphite crystals are readily cleaved to give flakes of suitable size for optical hot-stage and electron microscopy. Recent studies of the microtopographical features of these reactions have led to substantial progress in understanding the atomistics of the elementary processes and to an appreciation of the role of crystal defects as preferred sites for chemical attack. This information is very pertinent to an understanding of the chemical stability of the newer forms of carbon which have been discussed in earlier sections of this report.

The application of optical microscopy to the study of surface changes during oxidation of graphite single crystals was first developed by Hennig in the period 1959-1965. This was followed by the now classical investigations of Thomas, who was able to measure directly the anisotropy of the reaction in different crystallographic directions and to identify the special importance of crystal defects, pre-eminently nonbasal dislocations, in determining the preferred sites for attack on the graphite basal plane surface. This fascinating work has been summarized in a comprehensive review.[131]

In brief, the oxidation of graphite single crystals in oxygen causes rapid gasification of edges and surface steps, but also the formation of etch pits at dislocation cores in the basal plane. This localized reaction at basal plane defects is an inherent feature of graphite oxidation and cannot be solely attributed to impurities. However, because of the ever-present contaminants trapped in dislocation cores, it is not possible to correlate the enhanced localized reactivity with the energetics of the dislocations. In passing it may be noted that many metallic impurities, especially oxides, are strong catalysts for graphite oxidation,[84] whereas compounds of phosphorus and halogens are often oxidation inhibitors.[132] When the uncatalyzed oxidation is carried out below about 900°C, the resultant etch pits are invariably hexagonal in form and oriented such that two of the pits sides are parallel to the $\langle 10\bar{1}0\rangle$ twin bands that thread the crystal. A parallel pit of this type is shown schematically in Fig. 14(A). Alternatively, when the oxidation is carried out above 1000°C, the pits have a perpendicular orientation, depicted in Fig. 14(B). This result implies that the rate of oxidation in the $\langle 10\bar{1}0\rangle$ crystallographic directions is somewhat greater in the lower temperature range than in the $\langle 11\bar{2}0\rangle$ directions, whereas above 1000°C the reverse is the case. The arrangement of unsaturated C atoms on the pit sides is different in the two cases: the parallel pit having adjacent pairs of unsaturated C atoms, whereas the perpendicular pit has alternate C atoms with unsaturated valencies. These labile carbon atoms are more likely to act as sites for chemisorption and reaction than are the more tightly bonded atoms at the pit corners. Experience with ball models soon shows, however, that it is not possible to maintain a given pit orientation by a random abstraction process of labile C atoms of one type.

The orientation of etch pits at dislocation cores is also strongly affected by the nature of the reacting gas. Thus hexagonal etch pits produced by atomic hydrogen at 700° to 800°C are of the perpendicular type, whereas nitrogen atoms at temperatures above 1000°C give exclusively parallel pits.[133] Roughly circular pits have been reported in the reaction of

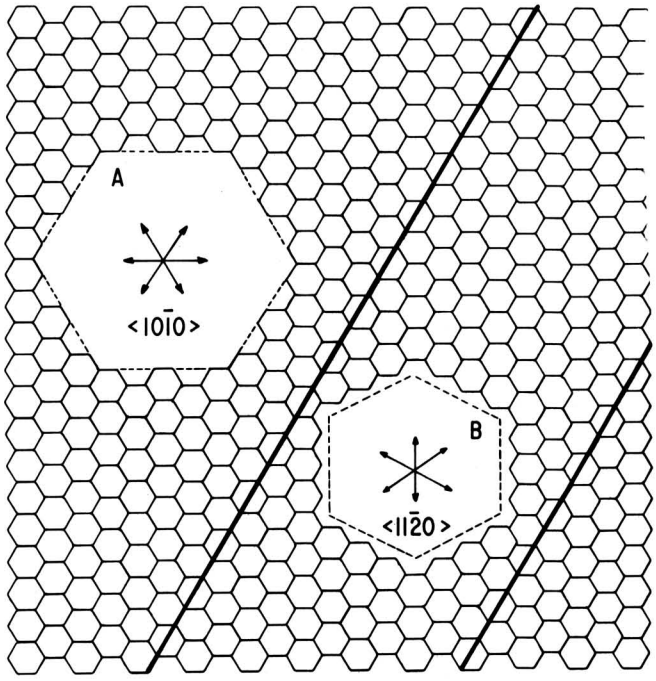

Fig. 14 Schematic arrangement of "parallel" A, and "perpendicular" B etch pits on basal plane of graphite. Dark parallel lines represent twin bands [from McKee(84)].

graphite crystals with moist air at 620°C,(134) implying that the reaction rate in this case is almost identical in the $\langle 10\bar{1}0\rangle$ and $\langle 11\bar{2}0\rangle$ directions. By contrast, atomic oxygen produced in a microwave discharge or from the thermal decomposition of ozone causes general erosion over the whole basal plane surface.(131)

Although optical microscopy yields fundamental information on the anisotropy of the gasification reactions, it fails to give insight into the processes occurring on an atomic scale. A more powerful technique for microtopographical studies, again originally developed by Hennig, has been the recent application of gold decoration to render etch pits visible in the electron microscope. By this method individual vacancies in the basal plane can be developed as circular rings, one atomic layer deep after etching in oxygen. The rings are enlarged to a diameter of about 1000Å and then gold is deposited to decorate preferentially the borders of the depressions. The method is capable of detecting a single surface vacancy in 10^{10} C atoms in the basal plane.

Using this technique, it has been discovered(135) that vacancies are created in the basal plane surface of graphite during treatment with oxygen at temperatures around 1000°C. It appears that atomic oxygen, produced by thermal dissociation of O_2, is responsible for this vacancy formation. By measuring the rate of enlargement of the surface rings, Evans and Thomas(135) found that the activation energy for recession of the monatomic carbon layer (35 kcal $mole^{-1}$) is much less than that for recession of deep etch-pit edges formed in the vicinity of dislocation cores (62 to 67 kcal $mole^{-1}$), whereas the rate of oxidation in the monolayer is less by a factor of nearly 1000 than that of multilayer steps.(136) It is possible that this difference is a reflection of the strength of bonding of surface complex or chemisorbed oxygen in the two cases. CO_2 subjected to far ultraviolet photolysis is also capable of creating vacancies in the basal plane and radiolyzed CO_2 has a similar effect.(137) Montet and Myers(138) have used the gold decoration technique to study the kinetics of the reaction of graphite single crystals with water vapor and to determine the threshold energy required to displace a C atom from a site on the surface. By measuring the minimum energy required by electron irradiation to initiate the formation of vacancies, an energy of 31 eV was estimated.(139)

In the presence of water vapor the oxidation of vacancies sometimes gives hexagonal pits,(140) whereas dry oxygen normally forms only circular pits in the top C layer. A rather unconvincing attempt has been made to explain this difference on the basis of the abstraction of labile C atoms from preferred sites on the pit edges(141); however, the difference between the observed orientation of etch pits at dislocation cores and vacancies has not been satisfactorily explained, in spite of the fact that these differences could provide valuable clues to the elementary steps involved in the gasification reactions.

Recent application of high-energy photoelectron spectroscopy (ESCA) to the problem of oxygen chemisorption on graphite surfaces(142, 143) reveals that O atoms are almost exclusively held at edge sites on the prismatic and pyramidal faces of the crystallites, there being at least two different types of binding states involved. In this connection, attempts by Bennett, McCarroll, and Messmer(144) to apply molecular orbital theory to the calculation of chemisorption energies at different sites on the graphite lattice are of considerable interest. A semi-empirical quantum approach, based on the Extended Hückel Theory developed by Hoffman was initially used to estimate binding energies of H atoms at various sites on an idealized 16- and 32-carbon atom simulation of the graphite basal plane. The calculations included all valence electrons and overlap integrals, and self-consistent changes in binding energies were computed by an iterative adjustment of the adsorbate atom energy levels. An equi-binding energy surface for atomic H over a single hexagonal graphite cell is shown in Fig. 15, the numbers being calculated binding energies in eV. In this figure, positive energies correspond to binding. Although the absolute values of the energies are probably only crude approximations, the differences between the energies at different points in the lattice

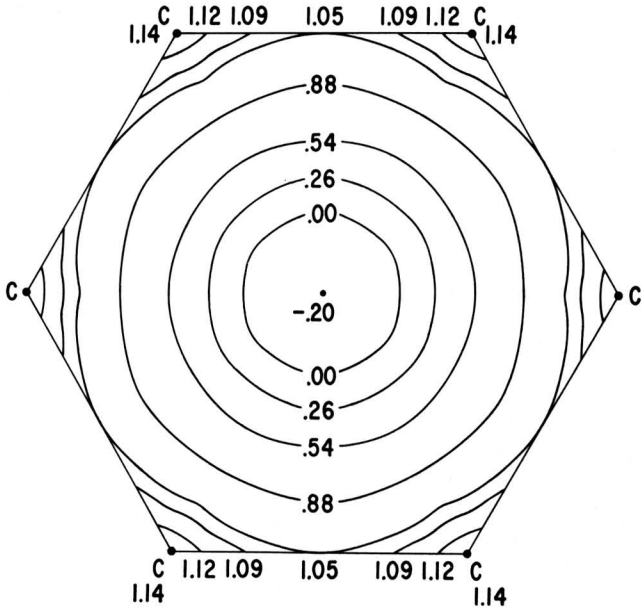

Fig. 15 Equi-binding energy contours (eV) for atomic H adsorbed on model (16C) graphite substrate [from Bennett, McCarroll, and Messmer(144)].

are significant. The maximum binding occurs above a C atom, although the barrier to H atom migration along the lines connecting nearest neighbor C atoms is small. It was also found that single H atoms bind with much higher energies (~4 eV) to edge C atoms than to those in the interior of the sheet, and it proved possible to compute the most stable configuration for successive additions of hydrogen atoms to edge C atoms. By this means it was shown that methane is the most energetically favored product of the graphite-hydrogen atom reaction.

Attempts to extend this treatment to electrophilic adsorbates such as N and O were, however, unsuccessful--as self-consistent adjustment of only the adsorbate matrix elements proved to be inadequate to ensure convergence. In a later paper, a more sophisticated approach, based on the CNDO (complete neglect of differential overlap) molecular orbital scheme of Pople, was used to calculate the chemisorption behavior of atomic H, C, N, O, and F on the graphite basal plane surface. This treatment led to the finding that the binding energy to the graphite substrate increased in the order H, F, O, N, and C. The atoms of C and N were most stable when positioned above the center of a hexagonal unit, whereas H, F, and O were most stable at mid-points of lines connecting nearest neighbor C atoms. A work function decrease was predicted for the chemisorption of H and N on graphite, but an increase for the chemisorption of C, O, and F. Although it is evident that the conclusions regarding binding sites are to some extent influenced by the assumptions and approximations involved in the model, it is likely that further refinements of this theoretical approach will lead to more quantitative information on the elementary steps involved in graphite gasification reactions, and on the effects of crystal defects on the energetics of chemisorption.

REFERENCES

1. Bacon, R. 1960. J. Appl. Phys. 31, 283.
2. Tesner, P. A., Robinovich, E. Y., Rafalkes, I. S., and Arefieva, E. F., 1970. Carbon 8, 435.
3. Robertson, S. D. 1970; ibid., p. 365.
4. Hillert, M., and Lange, N. 1958. Z. Krist. 111, 24.
5. Walker, P. L., Rakszawski, J. F., and Imperial, G. R. 1959. J. Phys. Chem. 63, 133.
6. Lieberman, M. L., Hills, C. R., and Miglionico, C. J. 1971. Carbon 9, 633.
7. Davis, W. R., Slawson, R. J., and Rigby, G. R. 1957. Trans. Brit. Ceram. Soc. 56, 67.
8. Patel, A. R., and Deshapande, S. V. 1970. Carbon 8, 242.
9. Baker, C. 1969. Carbon 7, 293.
10. Watt, W. 1972. Carbon 10, 121.
11. Watt, W. 1970. 3rd Conf. Ind. Carbon and Graphite, London.
12. Shionoya, I., Uchida, T., and Nukada, K. 1972. Carbon '72 Conf. Baden-Baden, 293.
13. Standage, A. E., and Matkowsky, R. 1969. Nature 224, 688.
14. Danner, B., and Meybeck, J. 1971. Plast. Inst. Intern. Conf. on Carbon Fibers, London.
15. Bailey, J. E., and Clarke, A. J. 1971. Nature 234, 529.
16. Morita, K., Miyachi, H., and Konoshita, Y. 1972. Carbon '72 Conf. Baden-Baden, 303.
17. Yamada, S., and Yamamoto, M. 1968. Carbon 6, 741.
18. Economy, J., and Lin, R-Y. 1971. J. Mater. Sci. 6, 1151.
19. Otani, S., Kokubo, Y., and Koitabashi, T. 1970. Bull. Chem. Soc. Japan 43, 3291.
20. Hawthorne, H. M., Baker, C., Bentall, R. H., and Linger, K. R. 1970. Nature 227, 946.

21. Boucher, E. A., Cooper, R. N. and Everett, D. H. 1970. Carbon 8, 597.

22. Johnson, D. J., and Tyson, C. N. 1970. J. Phys. Sec. D3, 526.

23. Johnson, D. J. 1970. Nature 226, 750.

24. Crawford, D., and Johnson, D. J. 1971. J. Microscopy 94, 51.

25. Johnson, D. J., Crawford, D., and Oates, C. 1971. 10th Carbon Conf., Bethlehem, Pa., FC-18.

26. Johnson, J. W., Rose, P. G., and Scott, G. 1970. 3rd Conf. Ind. Carbon and Graphite, London.

27. Williams, W. S., Steffens, D. A., and Bacon, R. 1970. J. Appl. Phys. 41, 4893.

28. Wicks, B. J. 1971. J. Mater. Sci. 6, 173.

29. Perret, R., and Ruland, W. 1970. J. Appl. Cryst. 3, 525.

30. Fourdeux, A., Perret, R., and Ruland, W. 1970. C. R. Acad. Sci. C271, 1495.

31. Fourdeux, A., Perret, R., and Ruland, W. 1971. 10th Carbon Conf. Bethlehem, Pa. FC-22.

32. Hugo, J. A., Phillips, V. A., and Roberts, B. W. 1970. Nature 226, 144.

33. Butler, B. L., and Diefendorf, R. J. 1969. 9th Carbon Conf. Boston, Mass., SS-25.

34. Watt, W., Johnson, W. 1970. 3rd Conf. Ind. Carbon and Graphite, London.

35. Jones, B. F., and Duncan, R. G. 1971. J. Mater. Sci. 6, 289.

36. Jones, B. F. 1971; ibid., p. 1225.

37. Barber, M., Swift, P., Evans, E. L., and Thomas, J. M. 1970. Nature 227, 1131.

38. Connell, G. L. 1971. Nature 230, 377.

39. Tuinstra, F., and Koenig, J. L. 1970. J. Composite Mater. 4, 492.

40. Larsen, J. V., Smith, T. G., and Erickson, P. W. 1971. Naval Ordnance Lab. Report NOLTR 71-165.

41. Saunderson, D. H., and Windsor, C. G. 1970. 3rd Conf. Ind. Carbon and Graphite, London.

42. Cooper, G. A., and Mayer, R. M. 1971. J. Mater. Sci. 6, 60.

43. Sarian, S., and Strong, S. L. 1971. Fiber Sci. Technol. 4, 67.

44. Reynolds, W. N. 1970. 3rd Conf. Ind. Carbon and Graphite, London.

45. Johnson, J. W., and Thorne, D. J. 1969. Carbon 7, 659.

46. Thorne, D. J. 1970. 3rd Conf. Ind. Carbon and Graphite, London.

47. Jones, W. R., and Johnson, J. W. 1971. Carbon 9, 645.

48. Perret, R., and Ruland, W. 1972. Carbon '72 Conf., Baden-Baden, 318.

49. Ezekiel, H. M. 1970. J. Appl. Phys. 41, 5351; 1970 Science 169, 178.

50. Robson, D., Assabghy, F. Y. I., and Ingram, D. J. E. 1972. J. Phys. D5, 169.

51. Soule, D. E. 1958. Phys. Rev. 112, 698.

52. Robson, D., Assabghy, F. Y. I., and Ingram, D. J. E. 1971. J. Phys. D4, 1426.

53. Allen, S., Cooper, G. A., Johnson, D. J., and Mayer, R. M. 1970. 3rd Conf. Ind. Carbon and Graphite, London.

54. Bullock, R. E., 1971. Radiation Effects 11, 107.

55. Murphy, E. V. and Jones, B. F. 1971. Carbon 9, 91.

56. Jones, B. F., and Peggs, I. D. 1971. J. Nucl. Mater. 40, 141.

57. Peggs, I. D., and Mills, R. W. 1971. 10th Carbon Conf., Bethlehem, Pa., RD-119.

58. Jones, B. F., and Peggs, I. D. 1972. Nature 239, 95.

59. Bullick, R. E. 1972. J. Mater. Sci. 7, 964.

60. Sharp, J. V., and Burnay, S. G. 1972. Carbon '72 Conf., Baden-Baden, 310.

61. McKee, D. W., and Mimeault, J. V. 1973. Chemistry and Physics of Carbon, P. L. Walker, Jr., ed., Vol. 8, Marcel Dekker, New York, p. 151.

62. Spencer, D. H. T., Hooker, M. A., Thomas, A. C., and Napier, B. A. 1970 3rd Conf. Ind. Carbon and Graphite, London.

63. Byrne, G. A., and Jeffries, R. 1971. Chem. Ind. 29, 809.

64. Mimeault, J. V., and McKee, D. W. 1969. Nature 224, 793.

65. McKee, D. W. 1971. Unpublished observations.

66. Sach, R. S., and Bromley, J. 1972. U. S. Patent 3,642,513.

67. McKee, D. W. 1971. German Offen. 2,119,805.

68. McKee, D. W. 1970. Carbon 8, 131.

69. Mimeault, V. J. 1971. ACS 161st National Mtg., Los Angeles. Abstr. ORPL-45.

70. Scola, D. A., and Brooks, C. S. 1970. Soc. Plastics, Ind. 25th Mtg., Washington, D. C.

71. Cass, R. A., and Steingiser, S. 1971 U. S. Patent 3,627,570.

72. Harris, B., Beaumont, P. W. R., and Moncunill de Ferran, E. 1971. J. Mater. Sci. 6, 238.

73. Goan, J. C., and Prosen, S. P. 1969. ASTM Special Tech. Publ. 452:3.

74. Mimeault, V. J., and McKee, D. W. 1971. 10th Carbon Conf., Bethlehem, Pa., FC-25.

75. Thorne, D. J., and Price, A. J. 1971. Fiber Sci. Technol. 4, 9.

76. Belinski, C., Diot, C., and Keraly, F. X., 1970. C. R. Acad. Sci. C271, 1025.

77. Brooks, C. S., and Scola, D. A. 1970. J. Coll. Interface Sci. 32, 561.

78. Scola, D. A., Golden, G. S., and Brooks, C. S. 1972. ACS 163rd National Mtg., Boston, Mass. Abstr. COLL-54.

79. Jackson, P. W., and Marjoram, J. R. 1968. Nature 218, 83.

80. Jackson, P. W., and Marjoram, J. R. 1970. J. Mater. Sci. 5, 9.

81. Barclay, R. B., and Bonfield, W. 1971. J. Mater. Sci. 6, 1076.

82. Perry, A. J., deLamotte, E., and Phillips, K. 1970. J. Mater. Sci. 5, 945.

83. Braddick, D. M., Jackson, P. W., and Walker, P. J. 1971. J. Mater. Sci. 6, 419.

84. McKee, D. W. 1970. Carbon 8, 623.

85. Galasso, F., and Pinto, J. 1970. Fiber Sci. Technol. 2, 303.

86. Jones, R. W. 1970. Composites 34.

87. deLamotte, E., Phillips, K., Perry, A. J., and Killias, H. R. 1972. J. Mater. Sci. 7, 346.

88. Fitzer, E., Mueller, K., and Schaefer, W. 1971. Chemistry and Physics of Carbon, P. L. Walker, Jr., ed., Vol. 7. Marcel Dekker, New York, p. 237.

89. Yamada, S. 1968. DCIC Report 68-2, Battelle Memorial Inst., Columbus, Ohio.

90. Fitzer, E., Schaefer, W., and Yamada, S. 1969. Carbon 7, 643.

91. Marsh, H., and Wynne-Jones, W. F. K., 1964. Carbon 1, 269.

92. Noda, T., Inagaki, M., and Yamada, S. 1969. J. Noncryst. Solids 1, 285.

93. Schmitt, J. L. (Jr.), and Walker, P. L. (Jr.), 1971. Carbon 9, 791.

94. Noda, T., and Inagaki, M. 1964. Bull. Chem. Soc. Japan 37, 1534.

95. Kakinoki, J. 1965. Acta Cryst. 18, 578.

96. Furukawa, K. 1964. J. Cryst. Japan 6, 101.

97. Perret, R., and Ruland, W. 1972. Carbon '72 Conf., Baden-Baden, 84.

98. Takahashi, Y., and Westrum, E. F. (Jr.) 1970. J. Chem. Thermodynam. 2, 847.

99. Jenkins, G. M., and Kawamura, K. 1971. Nature 231, 175.

100. Phillips, V. A. 1972. Private communication.

101. Ban, L. L., and Hess, W. M. 1971. 10th Carbon Conf. Bethlehem, Pa., SS-99.

102. Cowlard, F. C., and Lewis, J. C. 1967. J. Mater. Sci. 2, 507.

103. Jenkins, G. M., Kawamura, K., and Ban, L. L. 1972. Proc. Roy. Soc. London A327, 501.

104. Yamada, S., Sato, H., and Ishii, T. 1964. Carbon 2, 253.

105. Tsuzuku, T. 1964. Carbon 1, 511.

106. Taylor, R. E., and Kline, D. E. 1967. Carbon 5, 607.

107. Fischbach, D. B. 1971. Carbon 9, 193.

108. Tsuzuku, T., and Saito, K. 1966. Japan J. Appl. Phys. 5, 738.

109. Yamaguchi, T. 1963. Carbon 1, 47.

110. Fischbach, D. B. 1967. Carbon 5, 565.

111. Gray, W. J., Morgan, W. C., Cox, J. H., and Woodruff, E. M. 1972. Carbon 10, 236.

112. Marsh, H., and Rand, B. 1971. Carbon 9, 63.

113. Blackman, L. C. F., 1967. Carbon 5, 196.

114. Lewis, J. C., Redfern, B., and Cowlard, F. C. 1963. Solid State Electron. 6, 251.

115. Halpin, M. K., and Jenkins, G. M. 1968. Nature 218, 950.

116. Weisweiler, W., Subramanian, N., and Terwiesch, B. 1971. Carbon 9, 755.

117. Lewis, J. C., and Floyd, I. J. 1966. J. Mater. Sci. 1, 154.

118. Fischbach, D. B. 1971. Chemistry and Physics of Carbon, P. L. Walker (Jr.), ed., Vol. 7. Marcel Dekker, New York, p. 1.

119. Noda, T., and Kato, H. 1965. Carbon 3, 289.

120. Yokokawa, C., Hosokawa, K., and Takegami, Y. 1966. Carbon 4, 459.

121. Fitzer, E., and Kegel, B. 1968. Carbon 6, 433.

122. Gillot, J., Lux, B., Cornuault, P., and du Chaffaut, F. 1968. Ber. Deut. Keram. Ges. 45, 224.

123. El Goresy, A., and Donnay, G. 1968. Science 161, 363.

124. Whittaker, A. G., and Kintner, P. L. 1969. Science 165, 589.

125. Nelson, L. S., Whittaker, A. G., and Tooper, B. 1971. 10th Carbon Conf., Bethlehem, Pa., GS-208.

126. Stuckey, W. K., and Whittaker, A. G. 1971. 10th Carbon Conf., Bethlehem, Pa. TP-177.

127. Roberts, B. W., Diefendorf, R. J., and Marsh, H. Private communications.

128. Sladkov, A. M., Kasatochkin, V. I., Kudryavtsev, P. Yu, and Korshak, V. V. 1968. Izv. Akad. Nauk. SSSR, Ser. Khim. (Engl. trans.) 12, 2560.

129. Walker, P. L. (Jr.), Shelef, M., and Anderson, R. A. 1968. Chemistry and Physics of Carbon, P. L. Walker (Jr.), ed., Vol. 4, Marcel Dekker, New York, p. 287.

130. Lewis, J. B. 1970. Modern Aspects of Graphite Technology, L. C. F. Blackman, ed. Academic Press, New York, p. 129.

131. Thomas, J. M. 1965. Chemistry and Physics of Carbon, P. L. Walker (Jr.), ed., Vol. 1. Marcel Dekker, New York, p. 121.

132. McKee, D. W. 1972. Carbon 10, 491.

133. McCarroll, B., and McKee, D. W. 1971. Carbon 9, 301.

134. Lang, F-M., Gilles, P., Magnier, P., and Maire, P. 1966. J. Chim. Phys. 63, 1084.

135. Evans, E. L., and Thomas, J. M. 1970. 3rd Conf. Ind. Carbon and Graphite, London.

136. Evans, E. L., Griffiths, R. J. M., and Thomas, J. M. 1971. Science 171, 174.

137. Feates, F. S. 1968. Trans. Faraday Soc. 64, 3093.

138. Montet, G. L., and Myers, G. E. 1968. Carbon 6, 627.

139. Ibid. 1971. 9, 179.

140. Myers, G. E., and Gordon, M. D. 1968. Carbon 6, 422.

141. Feates, F. S. 1968. Ibid., p. 949.

142. Thomas, J. M., Evans, E. L., Barber, M., and Swift, P. 1971. Trans. Faraday Soc. 67, 1875.

143. Evans, E. L., Thomas, J. M., Boehm, H. P., and Marsh, H. 1972. Carbon '72 Conf., Baden-Baden, 49.

144. Bennett, A. J., McCarroll, B., and Messmer, R. P. 1971. Surface Sci. 24, 191; Phys. Rev. B3, 1397.